Highly selective Prins reaction over acid-modified halloysite nanotubes for synthesis of isopulegol-derived 2H-chromene compounds

Sidorenko, AYu; Kravtsova, AV; Aho, Atte; Heinmaa, I.; Wärnå, Johan; Pazniak, H.; Volcho, KP; Salakhutdinov, NF; Murzin, Dmitry; Agabekov, VE

Published in:
Journal of Catalysis

DOI:
10.1016/j.jcat.2019.05.009

Published: 01/01/2019

Document Version
Accepted author manuscript

Document License
CC BY-NC-ND

Highly selective Prins reaction over acid-modified halloysite nanotubes for synthesis of isopulegol-derived 2*H*-chromene compounds

A.Yu. Sidorenko*[1], A.V. Kravtsova[1], A. Aho[2], I. Heinmaa[3], J. Wärnå[2], H. Pazniak[4], K.P. Volcho[5,6], N.F. Salakhutdinov[5,6], D.Yu. Murzin*[2], V.E. Agabekov[1]

1 – Institute of Chemistry of New Materials of National Academy of Sciences of Belarus, 220141, Skaryna str, 36, Minsk, Belarus

2 – Åbo Akademi University, 20500, Biskopsgatan 8, Åbo-Turku, Finland

3 – National Institute of Chemical Physics and Biophysics, 12618, Akadeemia tee 23, Tallinn, Estonia

4– National University of Science and Technology "MISiS", Leninsky prospect, 4, 119049 Moscow, Russia

5 – Novosibirsk Institute of Organic Chemistry of Siberian Branch of Russian Academy of Sciences, 630090, Lavrentjev Av., 9, Novosibirsk, Russia

6 – Novosibirsk State University, 630090, Pirogova str. 1, Novosibirsk, Russia

Corresponding authors

Dr. A.Yu. Sidorenko

e-mail: camphene@gmail.com; Sidorenko@ichnm.basnet.by;

ph: +375 29 572 19 08

Address: Institute of Chemistry of New Materials of National Academy of Sciences of Belarus, 220141, Skaryna str, 36, Minsk, Belarus

Professor Dr. D.Yu. Murzin

Åbo Akademi University

Biskopsgatan 8, 20500, Turku/Åbo, Finland

ph: + 358 2 215 4985

e-mail: dmurzin@abo.fi

Graphical Abstract

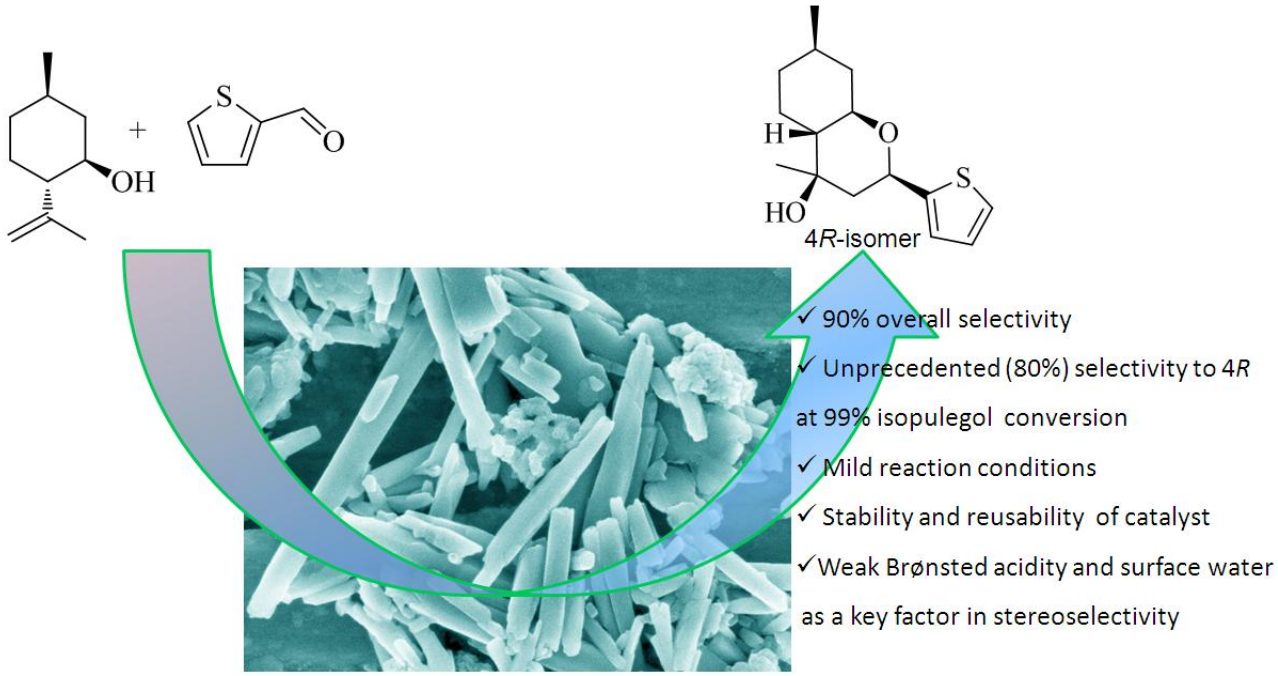

Highlights

Modified halloysite nanotubes as a stereoselective catalyst for synthesis octahydro-2*H*-chromen-4-ol

Unprecedented selectivity to target 4R isomer with analgesic activity at 99% conversion

Weak Brønsted acidity and surface water as a key factor in stereoselectivity

Stability and reusability of catalyst

Kinetic modelling

Abstract

Prins reaction of terpenoid (-)-isopulegol with thiophene-2-carbaldehyde giving in substituted octahydro-2*H*-chromen-4-ol (as 4*R*- and 4*S*-diastereomers) was studied for the first time over a series of halloysite nanotubes (Dragon Mine, USA), treated with 1 to 30% HCl. Materials have been characterized by MAS NMR, XRF, N_2 adsorption, FTIR with pyridine, SEM, TEM and thermal analysis methods. The quantitative data on the effect of acid treatment conditions on the content of structural units of halloysite are presented for the first time. The effect HNT treatment conditions, reaction temperature, catalyst loading, initial concentration of substrates on overall selectivity and 4*R*/4*S* ratio was studied. The diastereomers ratio decreased from 6.5 for air-dry nanotubes to 3.6 for counterparts dried at 350°C, which clearly indicates formation of 4R-isomer on weak Brønsted acid sites At 99% isopulegol conversion in cyclohexane over HNT treated with 5% HCl an unprecedented selectivity towards 4*R* alone (*ca*. 80%) was achieved close to the sum of both diastereomers on a commercial montmorillonite K-10. The 4*R*/4*S* ratio decreased with an increase in the concentration of acid sites. The excellent selectivity on halloysite was due to the predominance of weak acid sites. On the contrary, a low chromenols yield (*ca*. 30%) was observed over strong Brønsted acid (resin Amberlyst-15) related to direct formation of dehydration products from the substrates. Kinetic modelling shows a substantial difference in the order to the catalyst for the dried at 110°C resin (1.1±0.12) and air-dry halloysite (1.95±0.09) for the target 4*R*-isomer formation, which clearly indicates the key role of water in the reaction. A mechanism of isomers formation on HNT was proposed implying formation of an intermediate with the reagents and transfer of the surface water to the intermediate giving chromenols. Stability of the catalytic properties and reusability of HNT were demonstrated. Thus, modified halloysite nanotubes can be considered as a novel type of highly selective catalysts for the Prins reaction.

Keywords: Prins reaction, halloysite nanotubes, acid treatment, octahydro-2*H*-chromenol, chromenes, isopulegol, stereoselectivity, kinetic modelling, terpenoids

1. Introduction

It is known that compounds with a chromene (benzopyran) structure have a wide spectrum of physiological activity, such as anti-cancer, antiviral, analgesic, anti-inflammatory, etc. [1–7]. The high pharmaceutical potential and low toxicity of chromenes causes considerable interest in the synthesis and study of the properties of these substances [1–3, 8, 9].

To obtain benzopyran derivatives, typically, cyclization, cycloaddition and condensation reactions in the presence of various catalysts (Lewis and Brønsted acids, metals, complex compounds, etc.) are used [1–3]. Stereoselective synthesis of chromenes can be realized, for example, using chiral ligands [2]. Another approach involves catalytic reactions of optically active substances having an allylic alcohol fragment with carbonyl compounds [4].Thus, it was recently shown [10–12] that in the Prins reaction of commercially available natural terpenoid (-)-isopulegol (I) with aldehydes (II), substituted octahydro-2*H*-chromen-4-ols (III) are formed as 4*R*- and 4*S*-diastereomers along with dehydration by-products IV (Fig. 1).

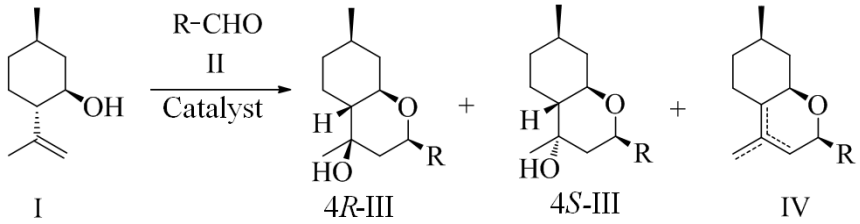

Fig. 1. A scheme of (-)-isopulegol reaction with aldehydes

A number of catalytic systems was proposed for the synthesis of chromenols III [10–17]. Thus, condensation of isopulegol with 4-methoxybenzaldehyde in the presence of iodine led to the formation of octahydro-2*H*-chromenols with a yield of 81% and 4*R*/4*S* diastereomers ratio equal to 5.0 [10]. In solventless reaction of compound I with propanal and isobutyraldehyde over *p*-TSA/SiO_2, chromenols III were formed with selectivity of 49 and 66%, respectively [11].

A relatively high value of 4*R*/4*S* (9.0) with a total yield of octahydro-2*H*-chromenols of 70–88% was observed in the Prins reaction of isopulegol (formed during cyclization of (*R*)-citronellal in reaction conditions) with aromatic aldehydes on scandium triflate at -78°C [12]. The diastereomers ratio was significantly lower (4.0) in the case of aliphatic aldehydes using [12]. In the presence of traditional Lewis acids ($ZnCl_2$, $AlCl_3$, $BF_3{\cdot}Et_2O$) a rather low yield of octahydro-2H-chromenols (12–48%) was observed [12, 13]. It should be noted that the utilization of homogeneous Lewis catalysts is associated with the difficulties of their separation from the reaction media, toxicity and, often, high costs (for example, in the case of triflates).

Modified zeolites Beta and silicates MCM-41 were investigated in the reaction of isopulegol with benzaldehyde [14]. The highest selectivity to chromenol III (83%) was observed in the presence of Ce-MCM-41 with a relatively low concentration of acid sites (a.s.). For zeolite Beta the overall selectivity to product III did not exceed 75% [14].

Acid-modified clay minerals are effective catalytic systems for the synthesis of octahydro-2*H*-chromenols [4, 7, 15–17]. Thus, the condensation of isopulegol with aromatic and aliphatic aldehydes over montmorillonite H-K-10 under microwave conditions led to formation of the target products III with yields of 50–86%. The reaction proceeded most selectively with 4-methyl- and 4-methoxy-substituted benzaldehydes [15]. It was shown that increasing the concentration of HCl to treat montmorillonite clay led to an increase in the catalyst acidity and a decrease in the ratio of desired (III) to side (IV) products in condensation of isopulegol with vanillin. In the presence of kaolinite activated with hydrochloric acid selectivity to chromenol was 76.8% with a vanillin conversion of 30% [17].

Many of the isopulegol-based octahydro-2*H*-chromene compounds have pronounced physiological activity [7, 13, 18, 19]. For example, 4*R*-diastereomer of chromenol III synthesized by condensation of I with thiophene-2-carbaldehyde on commercial K-10 clay (total isomers yield 78% with a 4*R*/4*S* ratio of 5.0) has a pronounced prolonged (24 h) analgesic effect superior to diclofenac used for comparison [7]. The 4*R*-isomers obtained by the reaction of isopulegol with acetone or 5-bromo-thiophen-2-carbaldehyde showed high antiviral activity, whereas the 4*S*-diastereomers had practically no antiviral effect [18, 19]. More recently, substituted octahydro-2*H*-chromen-4-ols containing nitrogen and sulfur atoms have been shown to be highly active as inhibitors of the Tdp1 enzyme, a promising target for antitumor therapy [20].

Considering a high pharmaceutical potential of chromenols, the development of effective methods for the stereoselective synthesis of these compounds is a very important task. Recently, our group for the first time established that in the reaction of isopulegol with thiophene-2-carbaldehyde on acid-modified illite clay, the yield of 4*R*-isomer increased with decreasing acidity of the catalyst and the reaction temperature, as well as by increasing the ratio of catalyst/reactants and initial concentration of the reagents [21]. Kinetic modelling was used to explain the observed regularities. It was shown that formation of by-products IV occurs both directly from the reagents and by dehydration of 4*R*-diastereomer (Fig. 2).

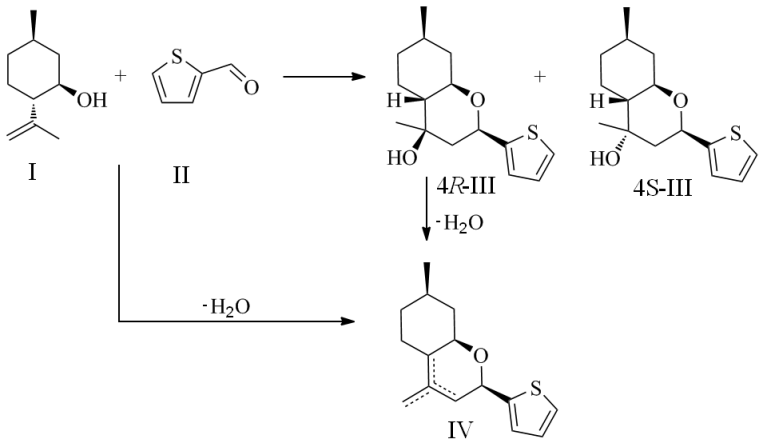

Fig. 2. The scheme of (-)-isopulegol reaction with thiophene-2-carbaldehyde

Halloysite is a clay mineral, the elementary layer of which is a combination of tetrahedral Si–O and octahedral Al–O sheets (Fig. 3). The two-layer packets of this mineral are bent into rolls and form multilayer aluminosilicate nanotubes, between the layers of which are water molecules [22–24]. Because of the significant potential for application of halloysite it has received a lot of attention [25]. This natural nanomaterial can be used as a container for drugs and protective agents delivery vehicle, in combination with polymers, membranes, biocompatible materials, etc. [22, 23, 26]. However, there are very few examples of halloysite-based materials utilization as acid catalysts [27–29].

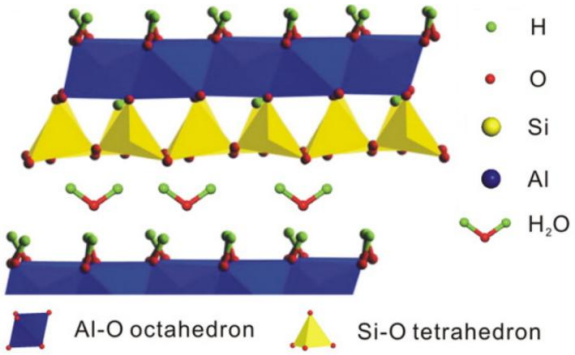

Fig. 3. Fragment of the halloysite structure

Recently, we have initiated utilization of halloysite nanotubes as catalysts for stereoselective synthesis of heterocyclic compounds via the Prins reaction [30]. As a result, it was reported in one preliminary communication that in the reaction of (-)-isopulegol with aliphatic and aromatic aldehydes octahydro-2*H*-chromenols are formed with excellent selectivity and a very high 4*R*/4*S* isomers ratio (7.6–14.5), significantly exceeding results on other types of catalysts [30].

Considering a very high potential of halloysite as a catalyst for synthesis of 2*H*-chromene derivatives, further research is extremely important, including optimization of HNT acid treatment,

catalyst characterization, optimization of the reaction conditions, and elucidation of reaction kinetics and catalyst reusability. In addition, a thorough comparison of the catalysts with different nature is necessary to better understand the role of HNT in the Prins condensation. The current study is devoted to investigation of (-)-isopulegol reaction with thiophene-2-carbaldehyde as an example. The choice of the aldehyde is related to a high analgesic activity of the resulting 4*R*-isomer.

2. Experimental

Preparation and characterization of catalysts

Commercially available halloysite from Dragon Mine (Utah, USA), which was purchased from Sigma-Aldrich, was used as the starting material for the catalysts preparation. Commercial acid-modified montmorillonite clays K-10 and K-30 (Germany), natural illite (IL) and synthetic aluminosilicate catalyst AS-36 (Russia) were used for comparison. In addition, the reaction was studied in the presence of Amberlyst-15 ion exchange resin (H^+-form, strongly acidic, total capacity ≥1.7 mol/l) and scandium triflate.

Catalysts K-10, K-30 and AS-36 were used as received. Acid treatment of halloysite was performed with a 1–30% hydrochloric acid solution. A certain amount of clay (10 g) was placed in a three-necked flask equipped with a reflux condenser and a thermometer. Thereafter a solution of HCl was added in the ratio of 5 ml per 1 g of HNT (5 ml/g), heated to 90°C and stirred at this temperature for 3 h, using a magnetic stirrer. The solid phase was then separated and washed from the acid with distillated water until complete absence of Cl^- (test with $AgNO_3$), dried on air at 105°C for 2 h, and then aged for 72 h at room temperature to attain air-dry material. For catalytic tests, air-dry halloysite was used, as well as dried immediately before the reactions at 50–350°C. A catalyst fraction of < 100 μm was used in all studies to avoid internal mass transfer limitation.

X-ray phase analysis of the halloysite and illite clays was carried out using a Dron-3 diffractometer (CuKα -radiation, $2\theta = 5–70^o$). The chemical composition of the samples was determined by X-ray fluorescence analysis, using the JEOL JED 2201 system (the analyzed elements were from B to U, the detection limit was 0.1%).

The images of halloysite were obtained with a scanning electron microscope Zeiss Leo 1530. A transmission electron microscope JEOL JEM-2100 with an accelerating voltage of 200 kV was used to study HNT. The samples were prepared by dropping halloysite dispersion onto a copper grid and dried in the air.

The porous structure of solids was measured with nitrogen physisorption on ASAP 2020 MP (Micromeritics) analyzer. The samples (*ca.* 50 mg) were previously evacuated (residual pressure 0.013 Pa) for 1 h at 200°C. The specific surface area was calculated by the Brunauer – Emmett–

Teller equation. The volume and the average diameter of the pores were determined from the desorption branch of the isotherm using the Barrett –Joyner–Halenda method [31].

^{29}Si MAS NMR spectra were recorded on Bruker AVANCE-II spectrometer in 8.5 T magnetic field using MAS probe for 10 mm zirconia rotors. Single pulse spectra were accumulated with 6 μs pulse (3/8 π) excitation at 71.43 MHz with a repetition time of 100 s at 5 kHz sample spinning speed. The chemical shifts are given in TMS scale.

^{27}Al MAS NMR spectra were recorded at 208.49 MHz on Bruker AVANCE-III spectrometer with 18.8 T external field using Bruker MAS probe and 3.2 mm zirconia rotors. The spectra were collected by a single 0.6 μs pulse (π/18) excitation with a repetition time of 1 s and 22 kHz sample spinning frequency. The spectra are referenced to the frequency of $Al(NO_3)_3$ solution.

Thermogravimetric analysis of halloysite was carried out with a Netzsch 449 F3 Jupiter thermal analysis system. The sample (*ca.* 60 mg) was heated from 30 to 900°C at a ramping rate 10°C/min in nitrogen recording the weight loss.

Acidic properties of the solids were determined by FTIR spectroscopy using pyridine as a probe molecule [32]. The samples were calcined at 350°C for 1 h, then cooled to 100°C and saturated with pyridine for 30 min. Total concentration of the weak, medium and strong acid sites was determined at 150°C. Medium and strong sites are related to ability of retaining pyridine at 250°C, while strong sites correspond to desorption at 350°C [33]. The identification of the Brønsted and Lewis sites was carried out for the absorption bands at 1545 cm^{-1} and 1450 cm^{-1}, respectively using the extinction coefficient of Emeis [34].

Reaction and analysis of products

Without solvent. 5 ml of dry methylene chloride were poured into a round bottom flask, 0.40 g (2.6 mmol) of isopulegol (Sigma-Aldrich, 98%), 0.29 g (2.6 mmol) of thiophene-2-carbaldehyde (Acros Organics, 98%), 0.10 g of n-decane (99.9%, internal standard) and contributed 0.69 g of catalyst. Methylene chloride was distilled off on a rotary evaporator at room temperature, the mixture was kept at 25°C for 1 h without stirring, after which the reaction products were extracted with ethyl acetate (3 x 7 ml x 10 min).

In solution. Cyclohexane was chosen as a solvent by reason of its lower toxicity compared with toluene and methylene chloride, used in several previous studies [10, 12, 17]. 5.0–50.0 ml of dry cyclohexane (Acros Organics, 99.9%) were poured into a three-necked flask equipped with a thermal controller and reflux condenser, equal amounts (2.6 mmol) of reagents, n-decane (0.1 g) were added and after reaching the required reaction temperature (20–60°C), a catalyst (0.35–1.38 g) was introduced. Stirring was carried out using a mechanical stirrer (600 rpm). Samples of the reaction mixture were periodically taken for analysis.

Composition of the reaction products was determined by gas chromatography using a Khromos GKh-1000 chromatograph with a flame ionization detector and a Zebron ZB-5 capillary column (30 mx 0.25 mm x 0.25 μm). The evaporator and detector temperature was 250 and 280°C respectively. Heating of the column from 110°C to 280°C was done with the ramp of 20°C/min, followed by the isothermal mode at 280°C. The total analysis time was 30 min.

The second order rate constants k were calculated from the following equation:

$$k=\frac{1}{t}\left(\frac{1}{c}-\frac{1}{c_0}\right)/\rho \qquad (1)$$

Where t, c and c_0 are the reaction time (s), current and initial concentration of reagents (mol/L) respectively and ρ is the catalyst bulk density (g/L).

3. Results and Discussion

3.1. Influence of acid treatment on composition, structure, morphology and acidity of halloysite

The diffractogram of the initial halloysite (Fig. 4) contains a typical set of peaks for this material with a characteristic maximum at 7.3Å and a shoulder at 10.0Å, which reflects the presence of water molecules between nanotubes layers [24, 35]. After treatment of halloysite by 30% HCl, a decrease in the intensity of all diffraction maxima is observed, which indicates a partial destruction of its crystalline structure. At the same time, no additional peaks are observed i.e. in the acid treatment of halloysite no new crystalline phases are formed. On a diffractogram of clay IL, a characteristic for illite set reflex is observed (Fig. S1, Supplementary Information).

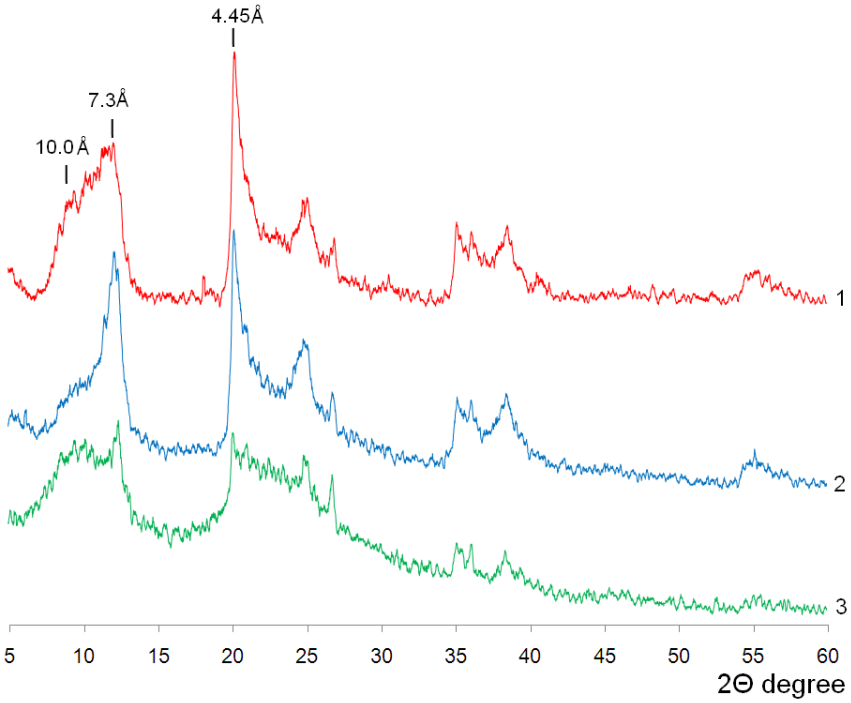

Fig. 4. X-ray diffraction patterns of the initial (1) and treated by 5% (2) and 30% (3) HCl halloysite

An increase in HCl concentration to treatment of halloysite from 1 to 30% results in a decrease in the amount of Al_2O_3 from 43.8 to 12.4 wt.%, and an increase in the content of SiO_2 from 55.1 to 87.0 wt.% respectively (Table 1). Note that HNT contains almost no iron and magnesium oxides, whereas in commercial montmorillonites K-10, K-30 and illite IL, their content was 1.4–6.4 wt.% (Table 1) as a consequence of the isomorphic substitution of $Fe^{2+/3+}$ and Mg^{2+} for Al^{3+} in the octahedral layers of these minerals [36, 37]. Note that the chlorine content in the samples was below the minimum detectable concentration i.e.<0.1%.

Table 1. Chemical composition and porous structure of the investigated solids

Material	Oxide content, wt.%								Porous structure		
	Al_2O_3	SiO_2	FeO	Na_2O	MgO	K_2O	CaO	TiO_2	S_{BET}, $m^2 \cdot g^{-1}$	V_{pore}, $cm^3 \cdot g^{-1}$	d_{pore}, nm
Halloysite initial	44.1	54.4	0.5	0.2	0.1	-	0.4	0.3	60	0.22	15.7
Treated by HCl solution, %											
1.0	43.8	55.1	0.4	0.1	0.1	-	0.2	0.3	62	0.25	16.8
5.0	39.9	59.1	0.4	0.1	0.1	-	0.1	0.3	129	0.34	11.3
10.0	32.1	66.9	0.3	0.1	0.1	-	0.1	0.4	167	0.40	10.1
20.0	18.3	80.9	0.2	0.1	0.1	-	0.1	0.3	189	0.59	13.0
30.0	12.4	87.0	0.1	0.1	0.1	-	0.1	0.2	207	0.65	13.1
IL	19.8	64.4	6.4	0.1	1.7	5.6	0.1	1.9	146	0.28	8.1
K-10*	14.5	77.1	4.0	0.1	2.0	1.2	0.4	0.7	247	0.36	5.1
K-30*	13.1	81.2	3.4	0.1	1.4	1.1	0.2	0.5	339	0.51	5.4
AS-36*	12.5	87.3	0.1	0.1	-	-	-	-	379	0.53	4.0

*The data from [33]

Low-temperature nitrogen adsorption isotherms for halloysite (Fig. S2) and illite (Fig. S3) are typical for mesoporous solids. The specific surface area (S_{BET}) of the initial HNT was 60 m^2/g and increased to 207 $m^2 \cdot g^{-1}$ after treatment with 30%. At the same time, an increase in the pore volume (V_{pore}) of halloysite from 0.22 to 0.65 $cm^3 \cdot g^{-1}$ (Table 1) is observed. Note that the value of S_{BET} for catalysts K-10, K-30 and AS-36 is significantly higher than for HNT. An increase in S_{BET} and V_{pore} during the acid treatment of layered aluminosilicates is associated with the removal of structural cations, partial disordering of their laminar structure and formation of amorphous silica [36, 37]. Halloysite was characterized by a pore diameter (d_{pore}) larger than montmorillonite and illite clays, while the smallest value d_{pore} was observed for the synthetic aluminosilicate AS-36 (Table 1).

In the FTIR spectrum of the initial halloysite (Fig. 5), in the region of 1400–900 cm^{-1}, a broad intense absorption band was observed at 1030 cm^{-1} with a shoulder of *ca.* 1090 cm^{-1}, associated with the stretching (ν) vibrations of Si–O in the structure [38]. The set of lines in the range of 700–400

cm^{-1} is assigned to bending (δ) vibrations of Si–O bonds, among which the peaks at 538 and 470 cm^{-1} belong to the Si–O–Al and Si–O–Si fragments, respectively [38]. The absorption band at 912 cm^{-1} is due to δ vibrations of the Al – OH groups [38].

With an increase of HCl concentration for halloysite treatment, a decrease in the intensity of the lines was observed at 1030, 912, 538 and 434 cm^{-1}, a shoulder appeared at 1180 cm^{-1}, and the absorption band at 470 cm^{-1} became wider. This indicates that a part of the Si–O–Al bonds are broken as a result of HNT acid treatment with the formation of Si–O–Si fragments. Absorption in the region of 1180 cm^{-1} is characteristic for Si–O –Si bonds in amorphous silica, which is the final product of the acid treatment of clays [36, 38].

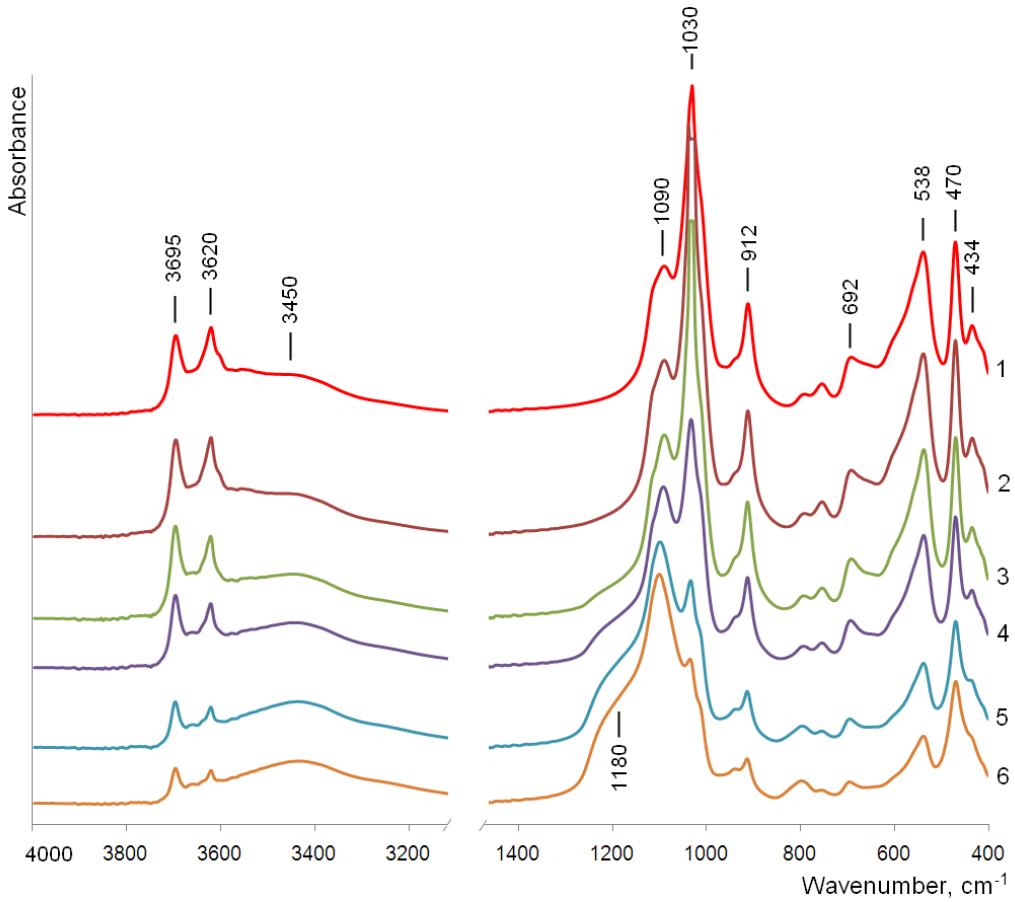

Fig. 5. FTIR spectra of halloysite initial (1), and treated by 1 (2); 5 (3); 10 (4); 20 (5) and 30% (6) HCl.

The peaks at 3695 and 3620 cm^{-1} in the FTIR spectra of halloysite (Fig. 5) correspond to the stretching vibrations of the structural –OH groups, and the broad band with a maximum at 3450 cm^{-1} is associated with the presence of adsorbed water molecules on the HNT surface [38, 39] . With increasing HCl concentration, a decrease in the intensity of the peaks was observed at 3695 and 3620 cm^{-1} and an increase at 3450 cm^{-1}. At the same time, the absorption significantly decreased at 912 cm^{-1} (δ (Al – OH)). Thus, removal of a part of Al^{3+} ions during acid treatment causes a decrease in

the number of structural hydroxyl groups because of crosslinking Si–OH fragments with formation of amorphous silica. An increase in the peak intensity at 3450 cm^{-1} (Fig. 5) after acid treatment of halloysite indicates an increase in the content of adsorbed water on the surface.

In Fig. 6 demonstrating thermal analysis data of the initial (TG-1), as well as treated by 10 (TG-2) and 30% HCl (TG-3) halloysite, the weight loss was observed in the intervals of 50–140 and 380– 560°C with maxima of the mass decrease rate (DTG curves) at *ca.* 80 and 510°C, respectively. The peak at 80°C is because of the loss of water adsorbed on the surface or between HNT layers, and a maximum at 510°C is associated with the removal of structural hydroxyl groups [24]. After acid treatment of halloysite, there is a slight increase in the intensity of the DTG-2 and DTG-3 curves at 80°C, while the peaks at 510°C are significantly diminished compared to that for the initial solid. This indicates a decrease in the number of structural –OH groups as a result of acid treatment of halloysite.

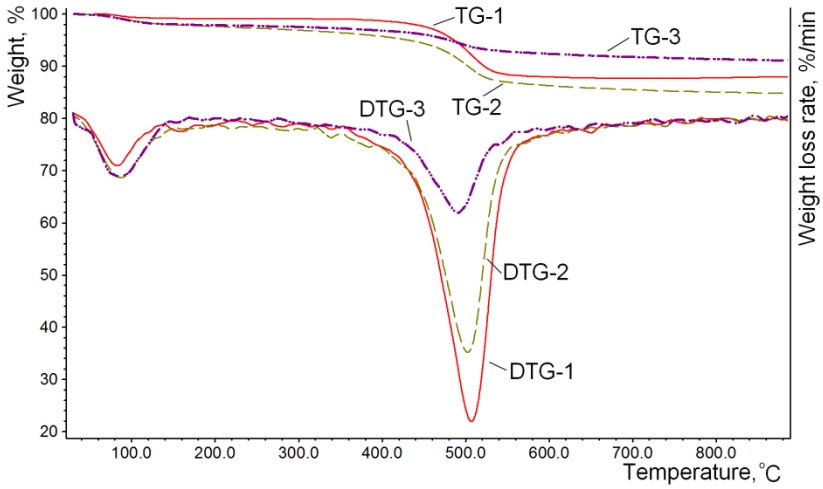

Fig. 6. Thermal analysis of halloysite initial (TG-1, DTG-1) and acid treated by 10% (TG-2, DTG-2) and 30% (TG-3, DTG-3) HCl

The ^{29}Si MAS NMR spectrum of the original halloysite nanotubes (Fig. 7) showed a single peak with a chemical shift (δ) at -91.8 ppm, which belongs to the Q^3 units, where one SiO4 tetrahedron is surrounded by three analogous ones [30, 40]. As a result of halloysite treatment with hydrochloric acid, additional signals appeared at -101.4 and -110.8 ppm. A line with δ = -101.4 ppm refers to the $(Si–O)_3Si–OH$ fragments [30], which are formed when the Si–O–Al bonds are broken between the tetrahedral and octahedral layers of halloysite. The peak with a chemical shift -110.8 ppm (Q^4(0Al) units) correspond to amorphous silica with a three-dimensional structure [40, 41], which is formed as a result of cross-linking of $(Si–O)_3Si–OH$, and is the final product of the acid treatment of clay minerals.

In the parent halloysite, 100% of Si^{4+} atoms are in Q^3 environment (Fig. 7). With an increase in the hydrochloric acid concentration from 1 to 30%, the content of these elements decreases from 94.2 to 15.7%. At the same time, the number of $(Si–O)_3Si–OH$ and Q^4 units increased, and after treatment of halloysite by 30% HCl, it was 20.5 and 63.8%, respectively (Fig. 7). Note that similar dependences were observed when Chinese montmorillonite was treated by sulfuric acid with different concentrations [42]. The current study for the first time presents quantitative data on the effect of acid treatment conditions on the content of structural units of halloysite.

Typical for acid-modified clay peaks at -92.0 (Q^3), -101.0 $(Si–O)_3Si–OH$ and -111.5 (Q^4) are observed in the ^{29}Si MAS NMR spectrum of hydrochloride-modified illite (Fig S4). The ^{29}Si NMR spectra of commercial montmorillonite K-10 and K-30 are described in detail in the previous work [33].

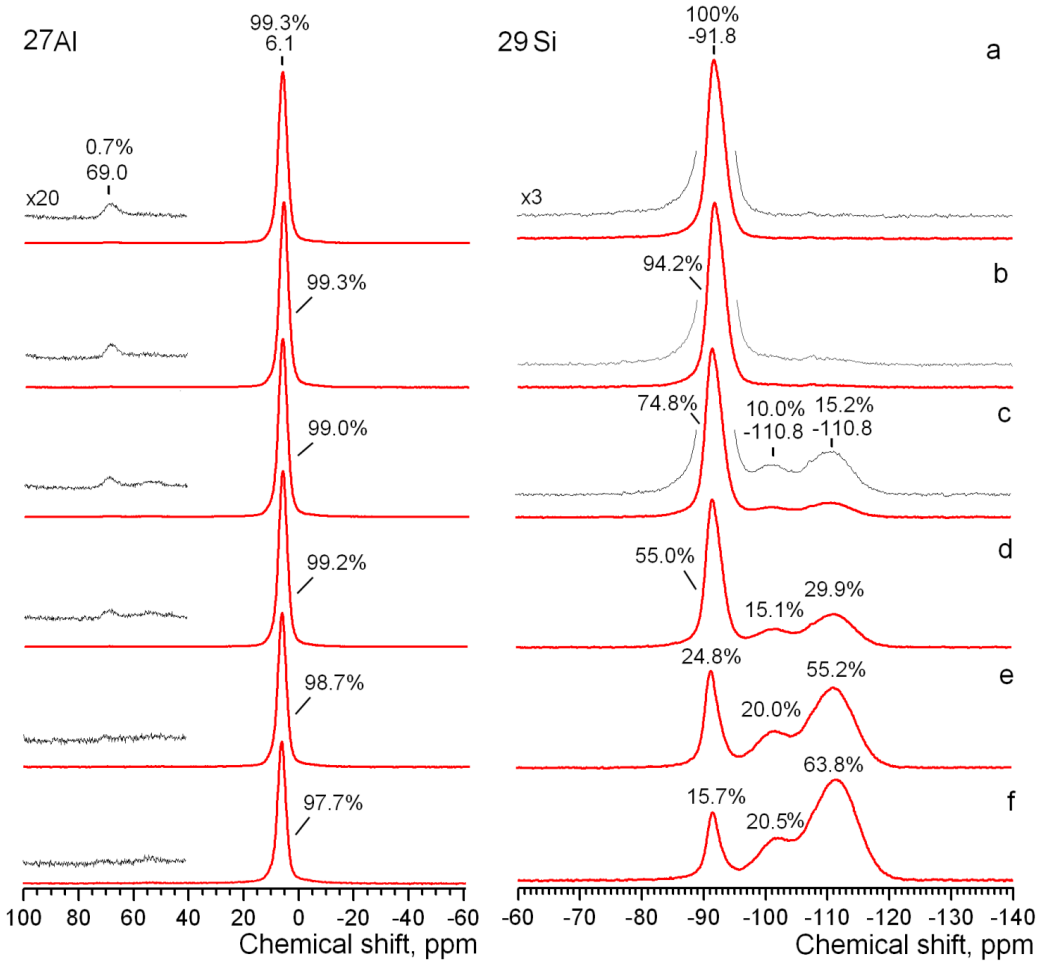

Fig. 7. ^{27}Al and ^{29}Si MAS NMR spectra of halloysite initial (a) and treated by 1 (b), 5 (c), 10 (d), 20 (e) and 30% (f) HCl

According to ^{27}Al MAS NMR spectrum, 99.0% of aluminum atoms in the initial HNT are in six-coordinated (Al^{VI}) state, i.e. in its octahedral layers [41]. The coordination state of aluminum

remains almost unchanged during the acid treatment of halloysite (Fig. 7), but its amount in the modified material decreased (Table 1). Unlike halloysite, 24.1% of Al^{3+} atoms in illite (Fig. S4) and 18–20% in montmorillonites K-10 and K-30 [33] are present in four-coordinated form as a result of the isomorphic substitution of Al^{3+} for Si^{4+} for in tetrahedral layers of these clays.

SEM images of halloysite (Fig. 8) exhibit cylindrical and prismatic nanoparticles with tubular morphology characteristic for Dragon Mine type of material [39]. Note that prismatic particles contain a kaolinite-like structure with 10 and 7.25Å interstratified layers [43], which is confirmed by the characteristic XRD pattern (Fig. 4). Images of HNT modified by 5 and 10% HCl (Fig. 8a, b) practically do not differ from those for the starting material (Fig. S6), whereas after treatment of nanotubes with 20.0–30.0% acid solution their significant destruction was observed (Fig. 8c, d).

According to transmission electron microscopy (TEM) data, an insignificant destruction, predominantly at the ends of the nanotubes, occurred already when they were pretreated with 5% HCl (Fig. 9a). Note that, according to ^{29}Si MAS NMR (Fig. 7), 15.2% of the silicon atoms in this sample are presented in amorphous silica (Q^4, -110.8 ppm). With increasing concentration of hydrochloric acid, destruction of nanotubes was more prominent, and the formation of spherical SiO_2 nanoparticles was observed (Fig. 9). This happens because of breaking the Si–O–Al bonds between tetra- and octahedral halloysite nanosheets, followed by cross-linking the $(Si–O)_3Si–OH$ structural units. Almost complete loss of the halloysite parent morphology occurred as a result of its treatment with 30% HCl (Fig. 9d), when more than 60% of Si^{4+} atoms were presented in amorphous silica.

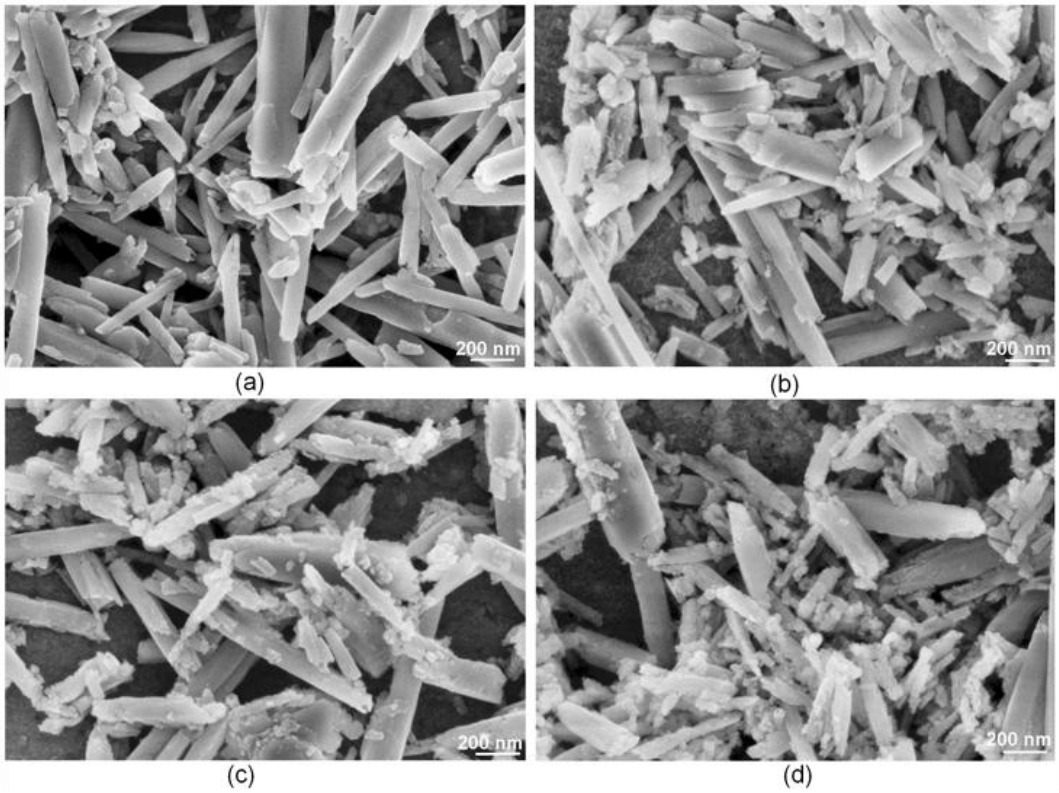

Fig. 8. SEM images of halloysite nanotubes treated with 5 (a), 10 (b), 20 (c) and 30% (d) HCl

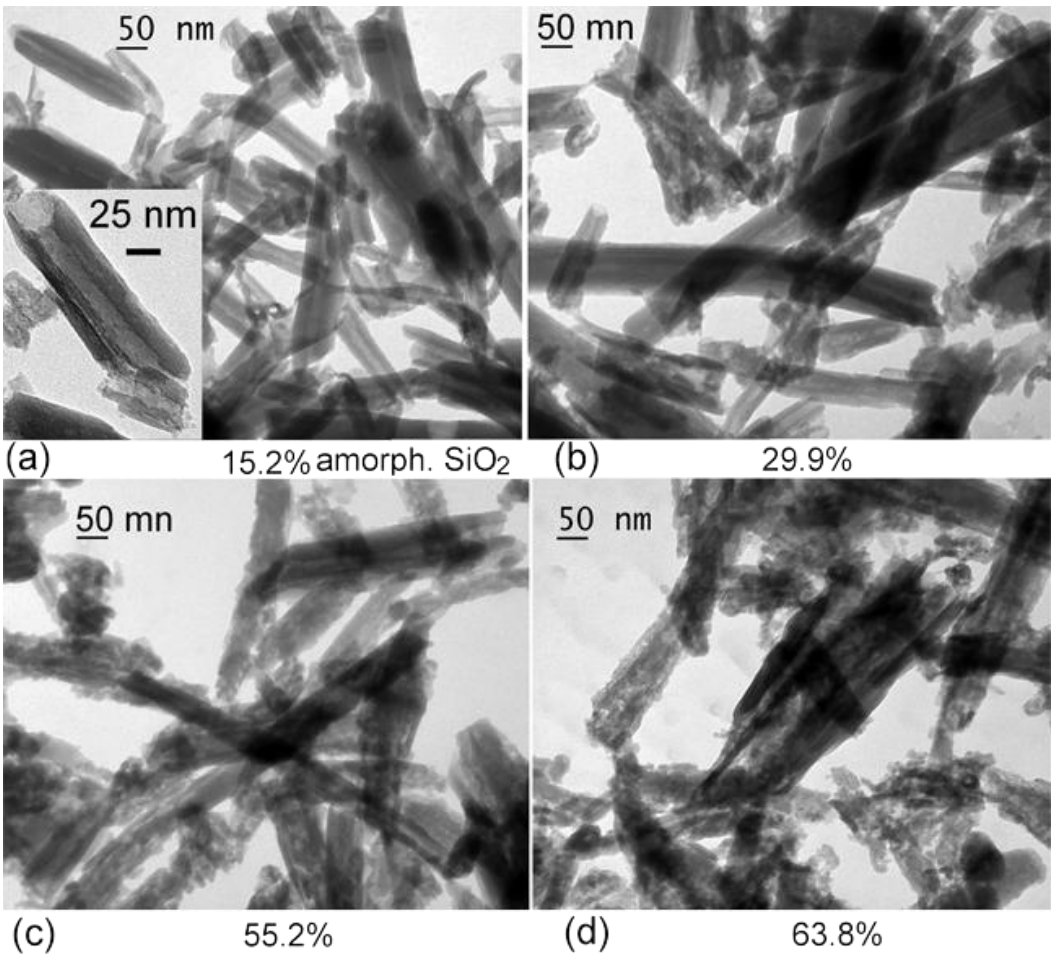

Fig. 9. TEM images of halloysite treated with 5 (a), 10 (b), 20 (c) and 30% (d) HCl (Percentage of amorphous silica from MAS NMR)

The concentration of acid sites (a.s.) on the halloysite surface increased from 34 to 52 μmol·g^{-1} after treatment with 10% HCl (Table 2). It is known that cationic exchange takes place under the action of acids on clays, which leads to an increase in their Brønsted (B) and Lewis (L) acidities [36]. In the initial and treated by 1–20% HCl halloysite, Lewis a.s. predominate (Table 2), while almost all aluminum atoms are in the six-coordinated state (Fig. 7). With an increase in the HCl concentration up to 30%, a sharp decrease in the concentration of a.s. (especially Lewis) was observed. This may be because of strong dealumination of solid [44], breaking of the Si–O–Al bonds, destruction of their structure and formation of amorphous silica, which is confirmed by the characterization of the samples by XRD, XRF, FTIR, MAS NMR, SEM, TEM and thermal analysis.

Table 2. Acidic properties of the investigated solids

Material	Acid site concentration, μmol·g^{-1}							L/B	$\frac{W}{M+S}$
	Brønsted (B)			Lewis (L)			Total		
	Weak (W)	Medium (M)	Strong (S)	Weak (W)	Medium (M)	Strong (S)			
Halloysite initial	12	1	-	17	4	-	34	1.6	5.8
Treated by HCl solution, %									
1	9	5	-	18	5	4	41	1.9	1.9
5	12	3	-	19	6	5	45	2	2.2
10	13	6	-	21	12	-	52	1.8	1.9
20	7	4	-	20	8	-	39	2.6	2.3
30	11	5	-	10	2	-	28	0.7	3.0
IL	11	16	-	12	14	11	53	1.0	0.77
K-10*	15	26	7	35	14	7	104	1.2	0.93
K-30*	17	17	8	28	24	6	100	1.4	0.82
AS-36*	34	31	16	32	21	19	153	0.9	0.76

*Acid sites concentrations and L/B ratio from [33]

Acidity of illite IL treated with 10% hydrochloric acid is close to that for HNT, exposed to HCl with the same concentration (Table 2), whereas the amount of a.s. in montmorillonites K-10, K-30 and aluminosilicate AS-36 is much higher. Difference in the acidity of the clays can be explained by peculiarities of their structure. Thus, as a result of isomorphous substitution of Al^{3+} for Si^{4+} in tetrahedral layers and metal cations with lower valency for Al^{3+} in the octahedral layers of clay minerals, a negative charge appears on their surface, which is compensated by exchange cations, including H^+. These ions are on the surface of the particles and in the interlayer space (Fig. S5). In the case of illite, the elementary layers are rigidly bound by K^+ ions, which are practically not subjected to cation exchange [45], which is the reason for lower acidity of this mineral compared to montmorillonites.

Isomorphous substitution of Al^{3+} for Si^{4+} in tetrahedral layers of halloysite was not observed, with *ca.* 99% of aluminum being in its octahedral sheets (Fig. 7). Thus, the total charge of its layers is balanced [36]. Therefore, Brønsted acid sites (H^+, acidic –OH groups, polarized water molecules) and Lewis (exchange and structural Al^{3+} cations) should be located mainly at the ends, splinters, and defects of the nanotube structure. The ratio of weak to the sum of medium and strong a.s. for halloysite is significantly higher than for other studied materials (Table 2). Thus, weak acidity prevails in HNT.

It is important to note that changes in the chemical composition, porous and crystalline structure, acidity and morphology of halloysite nanotubes can be effectively achieved by applying a

rather low ratio of acid to solid phase (5 mg per g), whereas in [40, 46, 47] for processing of 1 g HNT 100 ml of mineral (sulfuric, hydrochloric) or organic (acetic, acrylic) acids were used.

3.2. Catalytic activity of modified halloysite and comparison with other catalysts

3.2.1. Solventless conditions

Over the initial halloysite the Prins reaction of (-)-isopulegol I with thiophene-2-carbaldehyde II without any solvent was not observed. In the presence of acid-modified HNT for 1 h at 25°C the largest substrate conversion (*ca.* 83%) was observed after their treatment with 5–10% HCl (Table 3). A sharp decrease in the isopulegol conversion to 17.5% with an increase in acid concentration to 30% (Table 3) can be explained by a decrease in acidity (Table 2) and partial destruction of the catalyst structure (Fig. 9).

The main reaction product over modified halloysite was substituted octahydro-2*H*-chromen-4-ol III ((*2R,4R(S),4αR,7R,8αR*)-4,7-dimethyl-2-(thiophen-2-yl)-octahydro-*2H*-chromen-4-ol) as a 4*R* and 4*S* diastereomers. At the same time, there was a very high overall reaction selectivity (88.9–92.3%) with the 4*R*/4*S* ratio equal of 6.0–7.0. With an increase of HCl concentration for the halloysite treatment, there was a slight decrease in selectivity to both III and 4*R*-III (Table 3).

Table 3. Isopulegol conversion* (I) in reaction with thiophene-2-carbaldehyde and product selectivity** on acid-modified halloysite

Halloysite treated by HCl solution, %	Conversion (I), mol. %	Selectivity, mol. %				*4R/4S*
		III	*4R*-III	*4S*-III	IV	
1	36.0	92.3	80.8	11.5	3.3	7.0
5	83.4	91.5	79.3	12.2	3.9	6.5
10	82.3	92.1	79.7	12.4	3.4	6.4
20	33.4	89.9	77.0	12.9	3.9	6.0
30	17.5	88.9	76.6	12.3	3.7	6.2

*Conversion of aldehyde was practically the same as for isopulegol; **Without any solvent for 1 h at 25°C, air-dry catalyst

Drying of halloysite treated with 5% HCl (which showed the highest conversion of isopulegol) at a temperature from 50 to 350°C, immediately before the reaction, significantly affected the yield of octahydro-2*H*-chromenol and the diastereomers ratio (Fig. 10). Thus, after 1 h of reaction the selectivity to product III and the value of 4*R*/4*S* for the air-dry catalyst were 83.4% and 6.5 and decreased to 76.3% and 3.6, respectively, after its preliminary drying at 350°C (Fig

10a,b). At the same time, an increase in the yield of dehydration products IV was observed from 3.9 to 7.2% (Fig.10c). With an increase in the drying temperature of halloysite to 350°C, its weight loss increased (Fig. 10d) because of adsorbed water removal [24]. A decrease in selectivity to III after drying of the catalyst clearly indicates the important role of water in formation of octahydro-2*H*-chromenol. A detailed discussion of these results is given below.

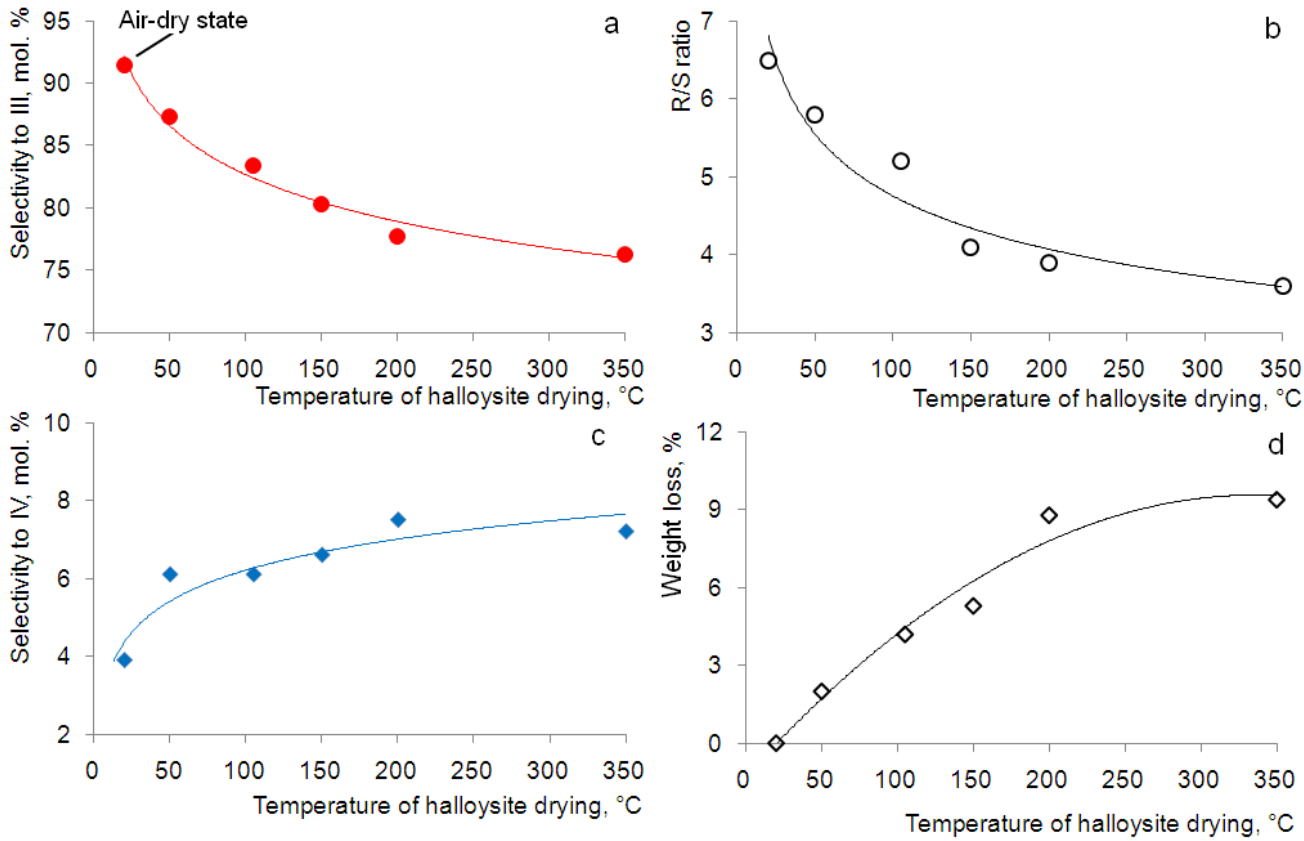

Fig. 10. Selectivity to products III (a) and IV (c), 4*R*/4*S* ratio (b) and catalyst weight loss (d) as a function of temperature of halloysite drying

3.2.2. In cyclohexane solution

Considering that the largest selectivity to the target 4*R*-III product was observed over air-dry halloysite nanotubes, all experiments were performed without drying the catalysts immediately before the reaction.

3.2.2.1. Effect of catalyst type and acidity

The Prins reaction of (-)-isopulegol with thiophene-2-carbaldehyde on modified HCl halloysite by 1–30% was carried out at 40°C according to [21, 30] using the initial concentrations of the reactants 0.5 mol/l in cyclohexane as a solvent.

Conversion of the substrate I after 6 h over the initial HNT was only 29.0% and increased to 56.8–99.0% after treatment of the catalyst with hydrochloric acid (Table 4). At the same time, almost complete conversion of isopulegol was observed in the presence of nanotubes treated with 5–10% HCl. For these samples the highest values of the second order rate constant *k* were observed (Table 4).

In the presence of halloysite catalysts a very high selectivity to chromenol III (89.3–91.3%) was observed. The 4*R*/4*S* ratio was the highest (6.8) in the case of HNT activation by 5% HCl (Table 4). Note that according to [21], the selectivity towards chromenol III decreased with an increase in the conversion of isopulegol due to subsequent conversion of compound III to IV. However, when using halloysite treated with 5% HCl, chromenol selectivity decreased only by 2% with an increase in the substrate conversion from 20 to 99% (Fig. S7).

Table 4. Isopulegol conversion and product selectivity on modified halloysite in cyclohexane *

Halloysite processed by HCl solution, %	$k \cdot 10^6$, $L^2 \cdot mol^{-1} \cdot s^{-1} \cdot g^{-1}$	Conversion (I), mol. %	Selectivity, mol. %				*4R/4S*
			III	*4R*-III	*4S*-III	IV	
Initial	0.26	29.0	91.3	79.3	12.0	4.5	6.6
1	1.8	85.2	90.6	78.6	12.0	6.8	6.6
5	3.1	99.0	90.7	79.0	11.7	6.3	6.8
10	3.2	98.1	89.4	76.8	12.6	7.8	6.1
20	1.1	80.6	89.3	77.1	12.2	6.8	6.3
30	0.78	56.8	90.4	78.5	11.9	5.6	6.6

*Conditions: initial concentration of isopulegol 0.5 mol/l, temperature 40°C, reaction time 6 h, air-dry catalyst

The overall reaction selectivity to octahydro-2*H*-chromen-4-ol in the presence of halloysite nanotubes modified by 5% HCl was significantly higher than on illite IL, montmorillonites K-10, K-30, and aluminium silicate AS-36 (Table 5). Moreover, selectivity of the 4*R*-diastereomer alone on HNT was comparable to that for the sum of both 4*R*- and 4*S*-isomers on commercial catalysts K-10 and K-30. The reaction rate constant *k* for HNT, IL, K-10 and K-30 linearly increased with increasing a.s. concentration (Fig. 11), whereas a rather low *k* value for AS-36 may be because of the presence of micropores [30].

Table 5. The products selectivity* in the reaction of isopulegol with thiophene-2-carbaldehyde**

Catalyst	$k \cdot 10^6$, $L^2 \cdot mol^{-1} \cdot s^{-1} \cdot g^{-1}$	Time, min	Selectivity, mol. %				*4R/4S*
			III	*4R*-III	*4S*-III	IV	
HNT	3.1	360	90.7	79.0	11.7	6.3	6.8
IL	7.2	360	83.9	71.4	12.5	11.3	5.7
K-10	15.3	180	81.5	66.1	15.4	10.7	4.3
K-30	10.8	180	81.6	66.5	15.1	10.5	4.4
AS-36***	1.2	540	79.4	61.6	17.8	11.7	3.5
Scandium triflate****	-	180	45.2	34.9	10.3	38.6	3.4

*At 99% conversion; *Conditions: initial concentration of isopulegol 0.5 mol/l, temperature 40°C, reaction time 6 h, air-dry catalyst; ***Only *ca.* 60% conversion was achieved; **** Conditions: CH_2Cl_2 as a solvent, temperature 20°C, isopulegol conversion was 67% after 3 h of the reaction

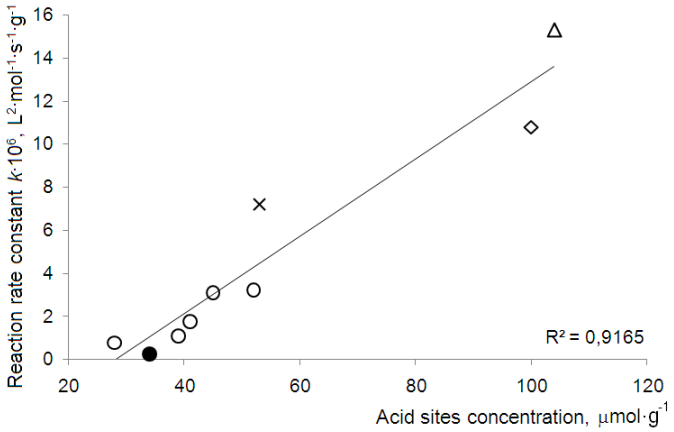

Fig. 11. Reaction rate constant as a function of acid sites concentration in catalysts (●–Initial and ○ – acid modified HNT; X – IL Δ – K-10; ◊ – K-30)

Considering that triflates showed high stereoselectivity in isopulegol condensation with aldehydes [12], but were not previously used in the case of thiophene-2-carbaldehyde, a control experiment using scandium triflate (5.0 mol. %) as a catalyst with a strong Lewis acidity was performed. After 3 h of the reaction the isopulegol conversion was 67%, giving low selectivity to octahydro-2*H*-chromen-4-ol (45.2%) with a 4*R*/4*S* ratio of 3.4 (Table 5). It should be noted that, according to [12, 13, 48], the use of typical Lewis acids ($ZnCl_2$, $AlCl_3$, $BF_3 \cdot Et_2O$) also resulted in rather low (12.0–48.0%) chromenols yields. Thus, using homogeneous catalysts with only Lewis acidity, acceptable yields of octahydro-2*H*-chromen-4-ols were not achieved.

Note that a combination of both weak Lewis and Brønsted acids as catalysts for the Prins reaction of 3-methylbutenol with aldehydes led to a sharp increase in their activity and selective formation of tetrahydropyran compounds [49]. Analysis of this synergy using the density functional

theory (DFT) showed that coordination of Lewis and Brønsted acids leads to an increase in their acidity [50]. In the present study, a rather high selectivity to octahydro-2H-chromenols (Table 5) was observed for all investigated catalysts exhibiting both Brønsted and Lewis acidity.

It was previously shown that the yield of the thiophenyl-substituted 4*R*-diastereomer was 65% on commercial montmorillonite K-10 without any solvent [6], 33% in the presence of an H-K-10 catalyst under microwave irradiation [11], and 69% on illite clay in cyclohexane [21]. An excellent yield (*ca*. 80%) of octahydro-2*H*-chromenol 4*R*-isomer with high analgesic activity was observed in the present study over modified halloysite nanotubes in cyclohexane at 40°C and 99% isopulegol conversion.

To understand differences in the catalytic properties of the solids studied, an analysis of the product selectivity as a function of acidity was performed. Because selectivity depends on isopulegol conversion [21], the comparison was carried out at the same (50%) substrate conversion.

In the original and modified halloysite the ratio of weak a.s. to the sum of medium and strong a.s. (W/(M+S)) was significantly higher than for other investigated solids (Table 2). At the same time, with an increase in the W/(M+S) value, an increase in the overall reaction selectivity to chromenol III (Fig. 12a) and its decrease to compounds IV (Fig. 12b) was observed.

Based on this, a high selectivity to chromenols (*ca.* 90%) in the presence of halloysite nanotubes can be assigned to the presence of weak a.s. in them. At the same time, domination of medium and strong acid sites in catalysts AS-36, K-10, K-30 and IL favors dehydration of compounds III into IV or direct formation of IV from the starting compounds. It should be noted that in the reaction of isopulegol with vanillin, an increase in the yield of products IV occurred with an increase of the a.s. concentration in montmorillonite catalysts [16].

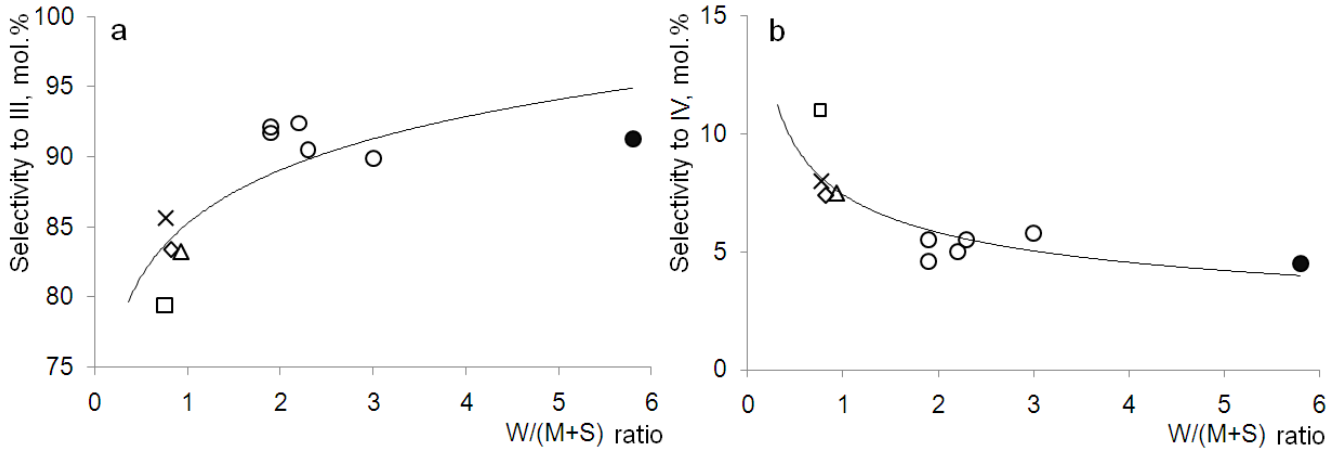

Fig. 12. Selectivity to products III (a) and IV (b) as a function of weak to the sum of medium and strong acid sites ratio (at 50% isopulegol conversion)
(●–Initial and ○ – acid modified HNT; X – IL Δ – K-10; ◊ – K-30; □ – AS-36)

Selectivity to the 4*R*-diastereomer of chromenol III decreased with increasing a.s. concentration on the catalyst surface (Fig. 13a). Thus, this isomer was most selectively (76.8–79.0%) formed in the presence of halloysite nanotubes with a relatively low concentration of acid sites (28–45 μmol·g^{-1}). An inverse relationship was observed for the 4S-isomer, the highest yield of which (17.8%) was achieved on AS-36 aluminosilicate with an acidity of 153 μmol·g^{-1}. The 4*R*/4*S* ratio also decreased with an increase in the concentration of a.s. in the catalysts studied (Fig. 13b). It is important to note that an increase in stereoselectivity (Table 5) was also observed with an increase in the ratio W/(M+S) (Table 2).

Thus, it can be concluded that a high yield of the target 4*R*-diastereomer in the reaction of isopulegol with thiophene-2-carbaldehyde over halloysite nanotubes is a result of both relatively low concentration and strength of acid sites.

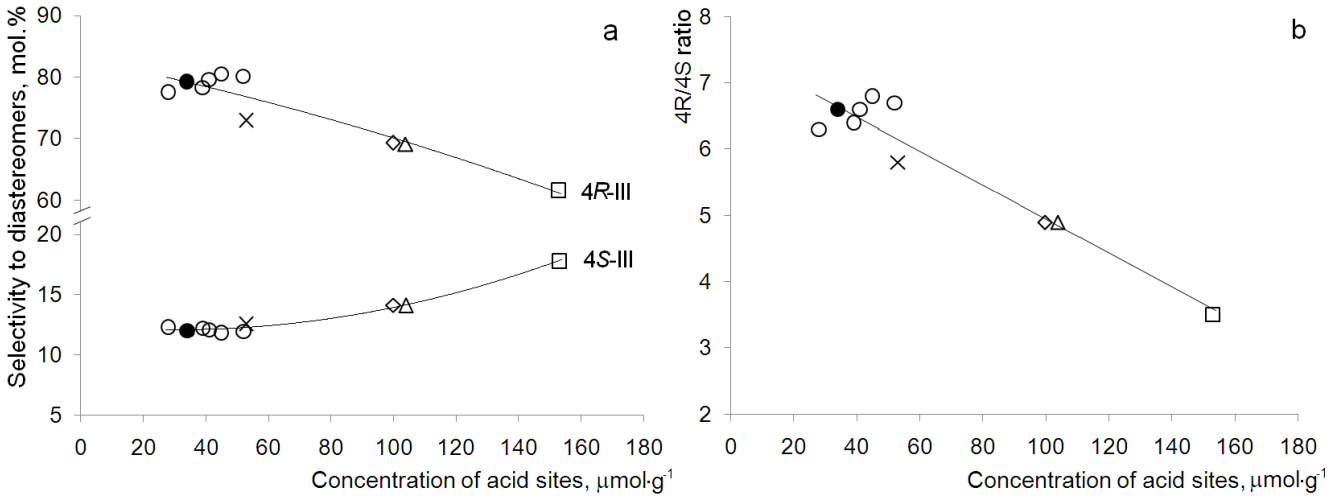

Fig. 13. Selectivity to diastereomers III (a) and 4*R*/4*S* ratio (b) as a function of acid sites concentration (at 50% isopulegol conversion)
(●–Initial and ○ – acid modified HNT; X – IL Δ – K-10; ◊ – K-30; □ – AS-36)

The increase in both overall selectivity to III and the 4*R*/4*S* ratio, observed when the drying temperature of halloysite nanotubes decreased (Fig. 10), can be explained by the change in the nature and strength of acid sites on their surface as a result of thermal treatment. Thus, the acidity of layered silicates is determined by exchangeable and coordination-unsaturated metal ions (Lewis a.s.), as well as acidic hydroxyl groups and water molecules linked to exchange cations (Brønsted a.s.) [36].

According to the ^{27}Al MAS NMR data (Fig. 7), almost all Al^{3+} atoms are in the six-coordinated state (in the octahedral layers of halloysite), i.e. isomorphous substitution is practically absent. Therefore, acid sites should be located predominantly at the ends and defects of the nanotube structure. In the parent and acid-treated halloysite Lewis a.s. prevail (Table 2). Water molecules present in nanotubes react with such sites: $[L(H_2O)_x]^{z+}=[L(OH)(H_2O)_{x-1}]^{z+-1}+H^+$, i.e. undergo

polarization and act as Brønsted a.s. [36]. It is known that the strength of these acid sites decreases with an increase in the cations hydration [36, 51]. In addition, the interaction of water with the clay surface leads to a decrease of the a.s. concentration [36].

Based on the above considerations, as the drying temperature increases, the surface dehydrated and the strength of acid sites in halloysite nanotubes increases. At the same time, a decrease in the 4*R*/4*S* ratio were observed (Fig. 10b). A key step in the mechanism of 4*R*- and 4*S*-isomers of chromenol formation (Fig. 14) is the addition of water to the intermediate cation III-A [7, 21]. The highest yield of 4*R*-diastereomer over air-dry HNT (79%) clearly indicates formation of this stereoisomer over the weak Bronsted a.s. (polarized H_2O molecules). This is fully consistent with an increase in both total and stereoselectivity with a decrease in the concentration and strength of acid sites (Fig. 12 and 13, Table 5). Because selectivity to 4*S*-isomer increases, and the 4*R*/4S ratio decreases with increasing a.s. concentration (Fig. 13), an increase in the catalyst acidity leads to a decrease in the ratio of the 4*R* to 4*S*-isomers formation rates.

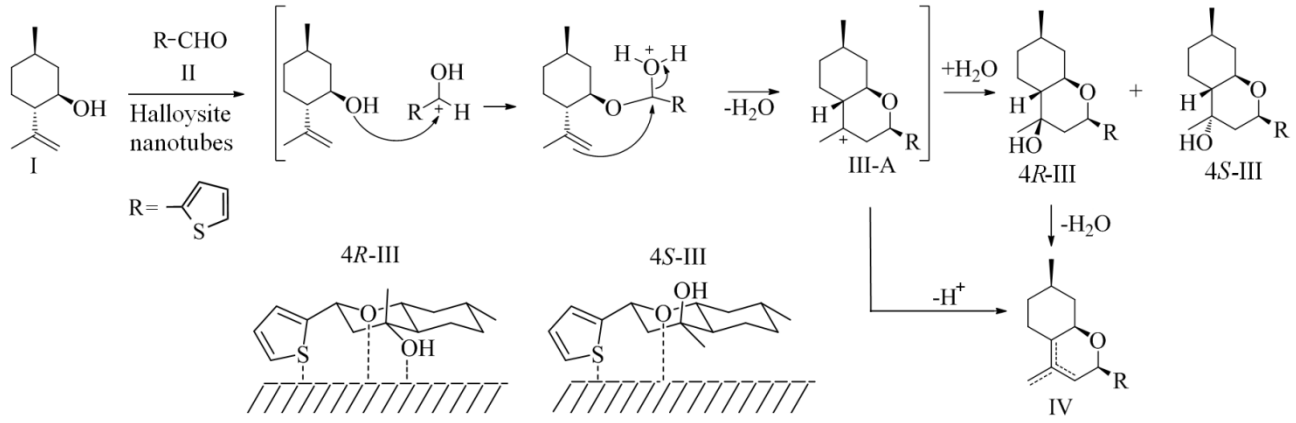

Fig. 14. The mechanism of (-)-isopulegol reaction with thiophene-2-carbaldehyde

On the other hand, an increase in the halloysite drying temperature or an increase in the W/(M+S) ratio in the catalysts led to an increase in selectivity to products IV (Fig. 10c and 12b). This indicates formation of compounds IV mainly on strong a.s. as a result of chromenol dehydration or directly from isopulegol and thiophene-2-carbaldehyde (Fig. 14). Note that, according to [21, 30], only the 4*R*-diastereomer undergoes dehydration, which can be explained on the basis of its spatial structure. Thus, interactions of this isomer with the catalyst surface may involve participation of the hydroxyl group, which leads to its removal (Fig. 14). In the case of 4*S*-isomer adsorption of the surface, the –OH group is probably directed in the opposite direction from surface, which makes dehydrate difficult. Considering that the active catalytic sites are located predominantly at the ends and defects of the nanotubes, condensation and dehydration reactions most probably occur only on the outer surface of halloysite.

3.2.2.2. Influence of initial concentration of reagents

With an increase in the initial isopulegol concentration in cyclohexane from 0.05 to 0.5 mol/l, selectivity to octahydro-2*H*-chromen-4-ol III (at substrate conversion of 50%) increased from 85.6 to 92.0%, respectively. The yield of dehydration products IV decreased from 11.4 to 4.9% (Table 6). This dependence indicates different molecularity of compounds III and IV formation on modified halloysite nanotubes. Thus, with an increase in the reagents concentration, the rate of the bimolecular chromenol III formation increases in comparison with the monomolecular dehydration III in IV [21, 52].

Table 6. Selectivity* over modified halloysite** at 50% isopulegol conversion

Isopulegol initial concentration, mol/l	Time, min	Selectivity, mol.%				*4R/4S*
		III	*4R*-III	*4S*-III	IV	
0.05	70	85.6	74.8	10.8	11.4	7.0
0.09	50	86.5	75.2	11.2	9.4	6.7
0.13	60	87.0	75.6	11.4	9.8	6.6
0.26	90	89.1	77.1	12.0	8.4	6.4
0.5	60	92.0	80.1	11.9	4.9	6.7

*Conditions: at 40˚C, initial concentrations of reagents were the same;**Treated by 5% HCl

It is important to note that at initial isopulegol concentrations of 0.5–0.26 mol/l, the reaction mixture became very viscous and decreased in volume after 60–80% substrate conversion, which made efficient stirring difficult. Therefore, for further analysis of the conditions and kinetic modelling, experiments were performed with an initial isopulegol concentration of 0.09 mol/l, when the above-mentioned phenomenon was absent.

3.2.2.3. Effect of reaction temperature

At 50% conversion of isopulegol an increase in the reaction temperature from 20 to 60°C led to a decrease in selectivity to chromenol III from 89.0 to 83.3% and subsequent increase to dehydration products IV from 6.6 to 10.7%, respectively (Table 7). At the same time, a decrease in the yield of only 4*R*-diastereomer was observed, while selectivity for 4*S*-III remained almost constant. As a result, the highest 4*R*/4*S* ratio (7.0) was achieved at 20°C (Table 7).

An increase in selectivity to the compounds IV with temperature elevation suggests that the activation energy of chromenol III formation is lower than for dehydration to products IV. Note that, according to [21], the activation energies for these consecutive reactions on illite clay were 82.0 and

90.7 kJ·mol^{-1}, respectively. The results of kinetic modelling of the Prins condensation of isopulegol with thiophene-2-carbaldehyde on HNT will be described below.

Table 7. Selectivity* over modified halloysite** at 50% isopulegol conversion

Reaction temperature, °C	Time, min	Selectivity, mol.%				*4R/4S*
		III	*4R*-III	*4S*-III	IV	
20	140	89.0	77.9	11.1	6.6	7.0
40	50	86.5	75.2	11.2	9.4	6.7
60	7	83.3	72.2	11.1	10.7	6.5

*Initial concentrations of isopulegol was 0.09 mol/l; **Treated by 5% HCl

Selectivity to chromenol III and compounds IV at 20 and 40°C on halloysite had a relatively weak dependence on isopulegol conversion, while at 60°C there was a sharp decrease in the yield of III with increasing conversion (Fig. S8). At the same time, selectivity towards 4*R*-III decreases with increasing isopulegol conversion, while it remains constant towards 4*S*-isomer. A sharp decrease in selectivity to 4*R*-III and its increase to the dehydration products IV was observed after 90% substrate conversion (Fig. 15a,b). Thus, on halloysite nanotubes, only the 4*R*-diastereomer undergoes dehydration, which may attributed to steric factors (Fig. 14). As a result of 4*R*-III secondary transformations, a decrease of the 4*R*/4*S* ratio was observed (Fig. 15c). Note that in the presence of illite clay at 60°C, the individual 4*R*-isomer was converted to IV products with 99% selectivity [21].

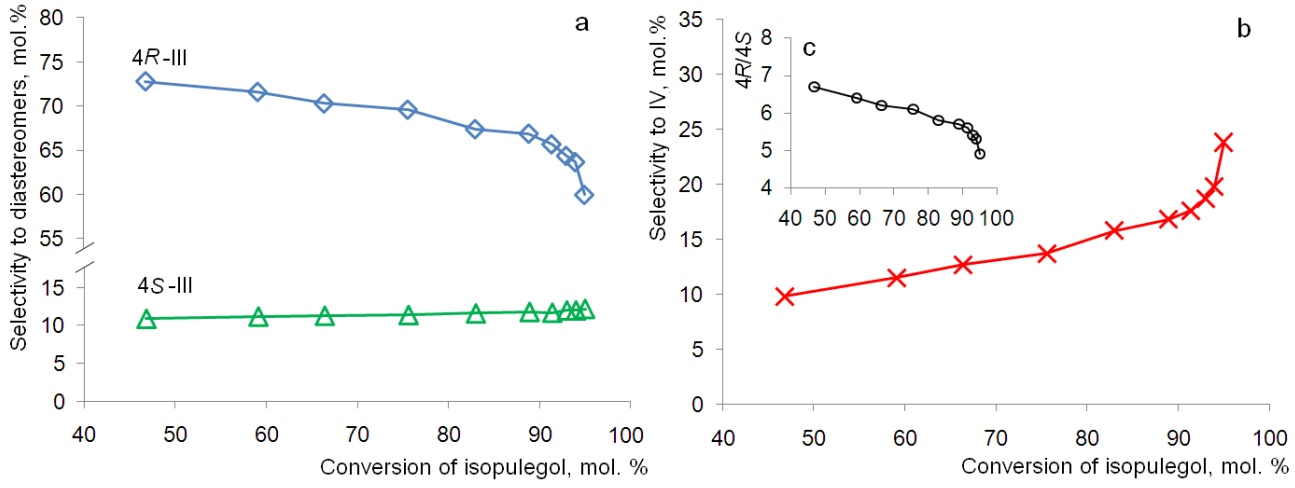

Fig. 15. Reaction selectivity to chromenol III diastereomers (a), dehydration products IV (b), and 4*R*/4*S* ratio (c) as a function of isopulegol conversion

3.2.2.4. Effect of the catalyst to reagents ratio

In the previously developed kinetic model of the isopulegol reaction with thiophene-2-carbaldehyde on illite clay, a second order towards the catalyst was observed for formation of both 4*R*- and 4*S*-diastereomers, which may indicate the involvement of water in the catalytic process [21]. At the same time, the overall yield and stereoselectivity in formation of octahydro-2*H*-chromenol had a strong dependence on the drying temperature of halloysite (Fig. 10). For a more detailed understanding of the role of H_2O on the catalyst surface, dependences of the products III and IV yields on the catalyst to reagent ratio were studied in the presence of air-dry halloysite (on the surface of which water molecules are present) and on Amberlyst-15 resin in H^+-form, dried to a constant weight at 110°C (when there was no water). The experiments were performed at 40°C and an initial isopulegol concentration of 0.09 mol/l.

In the presence of halloysite and Amberlyst-15, isopulegol conversion increased with an increasing amount of catalyst. Thus, for 3 h over HNT, conversion increased from 61.0 to 90.4% with an increase in the catalyst/reagent ratio from 0.5 to 2.0 (Fig. 16a). Over Amberlyst-15 for the same reaction time it increased from 80.8 to 99.0% (Fig. 16b).

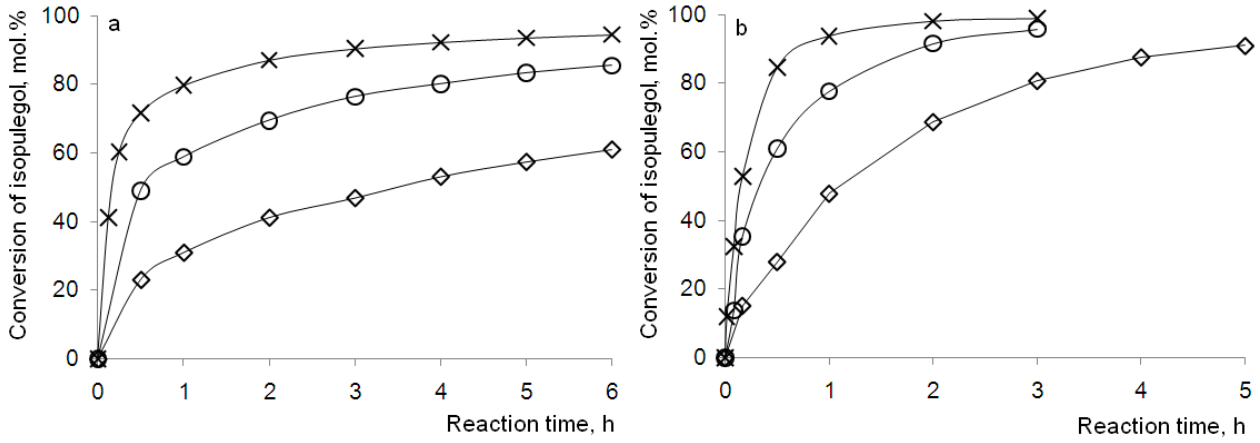

Fig. 16. Conversion of isopulegol over air-dry halloysite treated with HCl (a) and dried at 110°C Amberlyst-15 resin (b) as a function of reaction time at 40°C and initial substrate concentration 0.09 mol/l

(Catalyst to reagents ratio: ◊ – 0,5;○ –1,0;; X – 2,0)

According to the normalized time scale analysis [53], in the case of the first order reaction in the catalyst concentration, the substrate concentration curves as a function of $(m/n)\cdot t$ value (where m, n, and t are the catalyst mass, amount of the substrate, and reaction time respectively) should coincide. Fig. 17 shows that a satisfactory overlapping of the curves is observed only in the case of

Amberlyst-15 resin. Thus, condensation of isopulegol with thiophene-2-carbaldehyde in the presence of halloysite has a reaction kinetics deviating from the first order in the catalyst concentration.

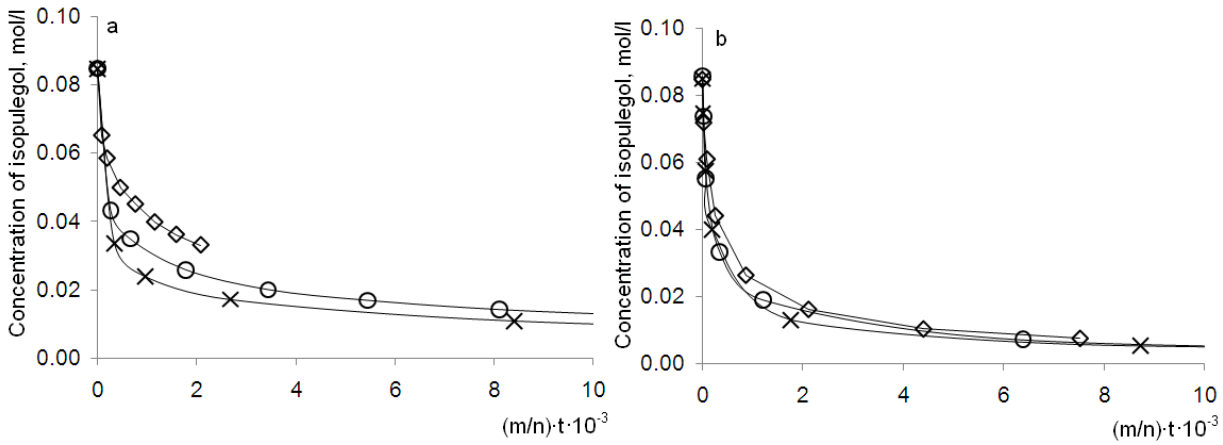

Fig. 17. Normalized time scale analysis for isopulegol condensation with thiophene-2-carbaldehyde over air-dry halloysite treated with HCl (a) and dried at 110°C Amberlyst-15 resin (b)

(Catalyst to reagents ratio: ◊ – 0,5;○ –1,0; X – 2,0)

Because formation of octahydro-2*H*-chromenol III is favored by a low concentration of acid sites, an increase in the catalyst/reagent ratio should lead to an increase in the number of acid sites participating in the reaction, and, accordingly, a decrease in selectivity to III. Indeed, on dry Amberlyst-15 at 60% isopulegol conversion, the selectivity to chromenol decreased from 30.7 to 24.3% and increased to dehydration products IV from 67.9 to 73.1% with an increase in the catalyst/reagents ratio from 0.5 to 2.0, respectively (Fig. 18a,b). However, on air-dry halloysite, an inverse relationship was observed, i.e. with an increase in the amount of catalyst, selectivity to octahydro-2*H*-chromenol III increased and decreased for compounds IV (Fig. 18a, b). The 4*R*/4*S* ratio was practically independent of the catalyst amount being, however, for halloysite, it was significantly higher than for Amberlyst-15 (Fig. 18c,d). It is important to note that a dramatic increase in the selectivity towards chromenol from 26.1 to 56.9% occurred when the reaction was performed on air-dry Amberlyst-15. These results clearly confirm participation of water present on the catalyst surface in the formation of octahydro-2*H*-chromenol.

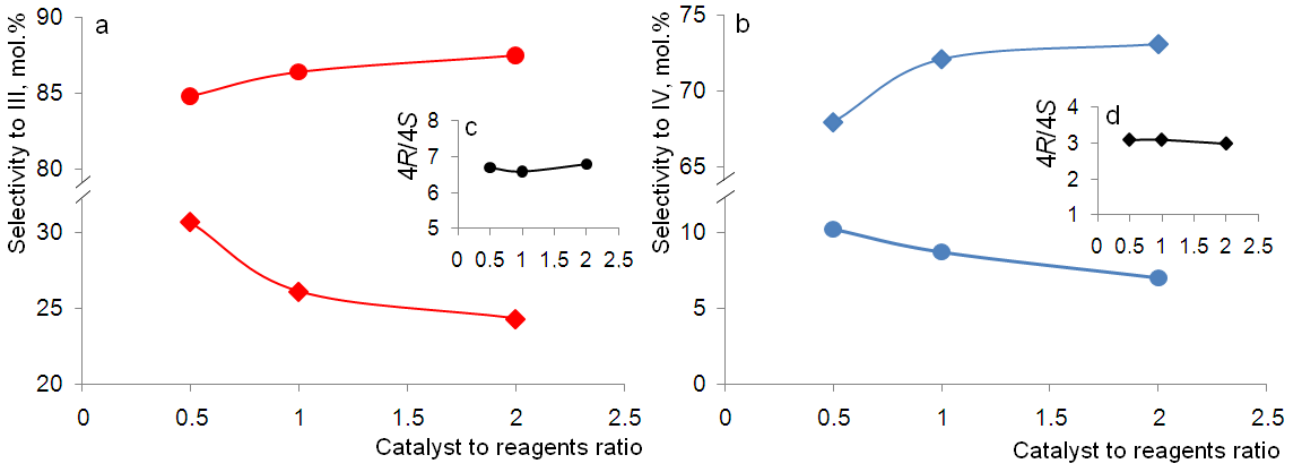

Fig. 18. Selectivity to products III (a) and IV (b), 4*R*/4*S* value (c, d) as a function of catalyst to reagents ratio at 60% isopulegol conversion

(● –air-dry halloysite; ♦ – Amberlyst-15, dried at 110°C)

According to the mechanism of isopulegol reaction with thiophene-2-carbaldehyde formation of 4*R*- and 4*S*-diastereomers occurs when H_2O is added to cation III-A (Fig. 14). In this case, an increase in the amount of water on the catalyst surface should lead to an increase of chromenol formation. Based on the spatial structure of this ion, its adsorption may be more preferred in a position in which the S and O atoms are directed closer to the catalyst surface, which leads to 4*R*-diastereomer formation (Fig. 19a). With increasing concentration and strength of acid sites, the selectivity for the 4*S*-isomer increases (Table 5, Fig. 13), which can be explained by the interaction of intermediate III-A with strong acid sites, in which the S and O atoms are more distant from the catalyst surface (Fig. 19b). A detailed quantum chemical study is required to confirm this hypothesis.

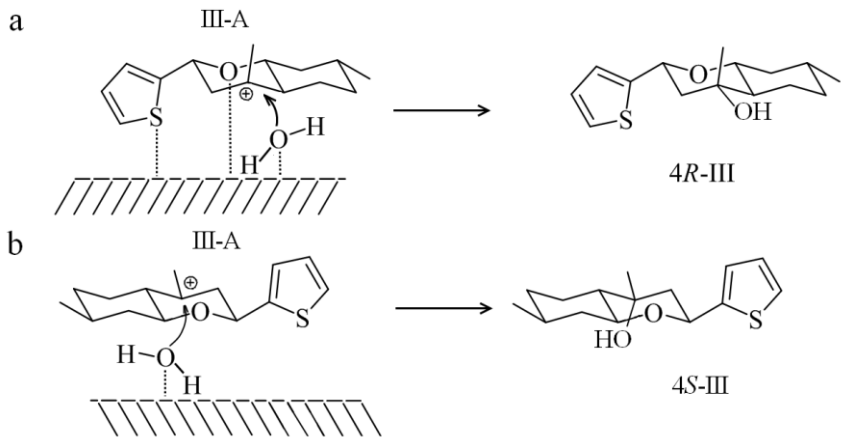

Fig.19. Scheme of the chromenol diastereomers formation by an interaction of water on the catalyst surface with an intermediate

The suggestion above points at also on the key role of water in the selective formation of 4*R*-diastereomer as a result of its interaction with intermediate III-A and an increase in selectivity for this isomer with a decrease in the drying temperature of halloysite nanotubes (Fig. 10). In this case, the addition of H_2O should be facilitated by their polarization due to interactions with acid sites [36]. Note that, according to [48], in the presence of the catalytic system $BF_3 \cdot Et_2O$ – H_2O, formation of 2*H*-chromene compounds with a fluorine atom in the position 4 was observed, which proves a possibility of a nucleophile (F^-) participation in the reaction by the mechanism similar to the one shown in Fig. 14.

3.3. Kinetic modelling

A kinetic model similar to the one previously reported by the authors for the Prins reaction of isopulegol with thiophene-2-carbaldehyde [21] was also applied in the current work. For the reaction network the scheme from Fig. 2 was utilized assuming that only 4*R*-III is dehydrated to product IV in line with a dependence of selectivity and 4*R*/4*S* ratio with conversion. The following kinetic equations were thus used for the modelling work:

$$r_1 = k_1 c_{iso} c_{ald} c_{cat}^{n_1};\ r_2 = k_2 c_{iso} c_{ald} c_{cat}^{n_2};\ r_3 = k_3 c_{4R} c_{cat}^{n_3};\ r_4 = k_4 c_{iso} c_{ald} c_{cat}^{n_4} \quad (1)$$

Where c_{iso}, c_{ald}, c_{4R} is the concentration of isopulegol, thiophene-2-carbaldehyde and 4*R*-diastereomer, respectively. Reactions 1 and 2 correspond to condensation of isopulegol with the aldehyde giving respectively 4*R*-III and 4*S*-III, while reactions 3 and 4 reflect formation of compound IV from 4*R*-III and by direct condensation of I and II, respectively. Similar to the previous considerations [21] the reaction orders in the catalyst concentration c_{cat} was deviating from unity.

The mass balances for the components are

$$\frac{dc_{iso}}{dt} = -r_1 - r_2 - r_4;\ \frac{dc_{4R}}{dt} = r_1 - r_3;\ \frac{dc_{4S}}{dt} = r_2;\ \frac{dc_{IV}}{dt} = r_3 + r_4 \quad (2)$$

The modified Arrhenius equation was used to account for the temperature dependence of the rate constant in the case of halloysite

$$k_j = k_{0j} e^{-\frac{E_j}{R}\left(\frac{1}{T} - \frac{1}{\bar{T}}\right)} \quad (3)$$

where E_j is the activation energy of a particular reaction step and $\bar{T}$ is the average temperature of experiments (K). The pre-exponential factor thus corresponds to the rate constant at the average temperature. A system of ordinary differential equations was solved with the backward difference method as a subtask to the parameter estimation with the Levenberg-Marquardt and/or Simplex

method with the software ModEst [54]. The estimated parameters are listed in Table 8 for halloysite and Amberlyst-15. The concentration curves shown in Fig. S9 and S10 confirm an adequate overall description of experimental data. The degree of explanation was 95.3% for halloysite and 98.7% for Amberlyst-15.

As can be seen from Table 8 the kinetic constants for the main reactions (formation of 4*R*- and 4*S*-isomers of III) were rather well identified being statistically reliable. The reaction orders in the catalyst were higher in the case of halloysite than for Amberlyst-15 as expected because the involvement of water in the clay surface is more prominent. Parallel – consecutive formation of compound IV through reactions 3 and 4 over halloysite gave a poorer statistical description, which can be related to much lower concentration of this compound compared to the main products. In the presence of Amberlyst-15 both kinetic constants for the diastereomers of III and products IV formation were statistically reliable which clearly indicates the immediate formation of IV from reactants on a catalyst exhibiting strong Brønsted acidity.

Table 8. Estimated kinetic parameters and their correlations

Parameter	Units	Halloysite*		Amberlyst-15**	
		Value	Error, %	Value	Error, %
k_1***	L h^{-1} $mole^{-1}$ $(L/g)^{n1}$	2.2 10^{-2}	28.0	1.3 10^{-3}	39.0
k_2***	L h^{-1} $mole^{-1}$ $(L/g)^{n1}$	1.7 10^{-4}	55.4	3.4 10^{-4}	73.1
k_3***	h^{-1} $(L/g)^{n1}$	1.5 10^{-3}	>100	4.1 10^{-5}	>100
k_4***	L h^{-1} $mole^{-1}$ $(L/g)^{n1}$	1.3 10^{-5}	>100	1.7 10^{-3}	17.4
Ea_1	kJ/mol	55	3.8	-	-
Ea_2	kJ/mol	58	8.5	-	-
Ea_3	kJ/mol	12	>100	-	-
Ea_4	kJ/mol	86	18.3	-	-
n_1	-	1.95	4.6	1.1	10.6
n_2	-	1.49	11.8	1.2	19.3
n_3	-	0.04	26.6	1.5	89.4
n_4	-	2.1	>100%	1.5	3.7

*Air-dry; **Dried at 110°C before reaction; ***The values of rate constants correspond to the average temperature for halloysite and to 40°C for Amberlyst-15.

The activation energies for formation of diastereomers of III (55–58 kJ/mol) on HNT were significantly lower than those on clay L-1 (82.1–98.9 kJ/mol) with stronger acid sites [21]. Thus,

weakly acidic halloysite nanotubes direct the reaction in a more energetically favorable path. In [55], experimental work and theoretical calculations were used to interpret the effect of acid strength on the selectivity in the Prins condensation. In the presence of weak Brønsted acids, the formation of a C–C bond occurs through a low charge transition state with partial covalence of O–H bond in the catalyst due to an incomplete proton transfer, which results in high selectivity. Over strong Brønsted sites, a full ion-pairs was formed, leading to side reactions [55].

In a similar way, formation of chromenol III on weak acid sites of halloysite can occur through an energetically favorable transition state with a partial proton transfer. In the presence of strong Brønsted a.s. (Amberlyst-15) a full ion-pair may be formed. Subsequent deprotonation of the intermediate leads to a direct formation of compound IV (from cation III-A as shown in Fig. 14), which is confirmed by kinetic modelling (Table 8). In the case of HNT, kinetic modelling does not allow unequivocal confirmation of direct generation of IV as a kinetic constant is not statistically reliable, whereas formation of these products by dehydration of the 4*R*-isomer was confirmed experimentally (Fig. 15).

For 4*R*- and 4*S*-diastereomers formation on halloysite, the reaction order for the catalyst was 1.95 and 1.49, respectively (Table 8), which indicates that water stored on nanotubes is involved in reaction. This assumes a dual mechanism of the catalyst action, which implies formation of an intermediate with the reagents and simultaneous polarization of water on the surface, facilitating its addition to the intermediate as shown in Fig. 19. A lower order in the catalyst towards 4*S*-III formation can be explained by a less prominent role of halloysite in the transfer of water to III-A because of the specific structure of this intermediate (Fig. 19b). The order in the catalyst in the case of dried Amberlyst-15 was close to unity, which clearly indicates that water from the reaction medium is involved in the octahydro-2*H*-chromenol formation.

3.4. Stability and reusability of halloysite catalyst

To study stability of halloysite treated with 5% HCl after the reaction at 40°C and 0.5 mol/l of the initial substrate cobcentration, the catalyst was separated from the reaction mixture, washed with ethyl acetate (3x 7ml x 10 min) and distilled water, dried at 105°C and aged in air within 12 h before reuse. The isopulegol conversion over fresh halloysite after 5 h was 96.8% and decreased to 87.3% after the third cycle. The overall selectivity for chromenol III remained almost unchanged, while the 4*R*/4*S* ratio slightly decreased (Table 9). After three reaction cycles (5 h of each), the halloysite nanotubes were reactivated with 5% HCl at 50°C for 3 h, thoroughly washed from the acid, dried at 105°C, and kept for 12 h before carrying out the reaction. In the presence of a regenerated catalyst

isopulegol conversion and the chromenol yield practically did not differ from the first cycle (Table 9).

Table 9. Isopulegol conversion* and products selectivity in the presence of halloysite ** for 5 h

Halloysite utilization cycle	Conversion (I), mol. %	Selectivity, mol.%				*4R/4S*
		III	*4R*-III	*4S*-III	IV	
1 (fresh)	96.8	90.6	78.9	11.7	6.4	6.7
2	90.6	89.2	77.0	12.2	7.1	6.3
3	87.3	89.1	77.1	11.9	7.3	6.5
Reactivated	97.2	90.0	78.1	11.9	7.0	6.6

*Conditions: at 40˚C, isopulegol initial concentrations was 0.5 mol/l;**Treated by 5% HCl

A slight decrease in the specific surface area and pore volume of the catalyst was observed after using halloysite nanotubes in 1–3 cycles in isopulegol condensation with thiophene-2-carbaldehyde (Table 10). At the same time, the pore diameter remains practically unchanged, while catalyst acidity slightly increases (Table 10). This can be explained by the appearance of defects in the structure of nanotubes after the reaction. Note that the nitrogen adsorption isotherms for the spent and regenerated halloysite (Fig. S11) are typical for mesoporous materials and are similar in shape to those of the original HNT (Fig. S2). SEM and TEM images of the modified halloysite nanotubes after 3 reaction cycles (Fig. 20a,b) and after reactivation by HCl (Fig. 20c,d) practically do not differ from the fresh catalyst (Fig. 8a, 9a).

Table 10. Physico-chemical properties of halloysite nanotubes after utilization in the reaction

Halloysite, Treated by 5% HCl	Porous structure			Acid sites concentration, $\mu mol \cdot g^{-1}$
	S_{BET}, $m^2 \cdot g^{-1}$	V_{pore}, $cm^3 \cdot g^{-1}$	D_{pore}, nm	
Fresh	129	0.34	11.3	45
After reaction cycles:				
1	123	0.32	11.7	54
2	111	0.29	11.3	52
3	111	0.30	11.8	49
Reactivated	119	0.31	11.4	54

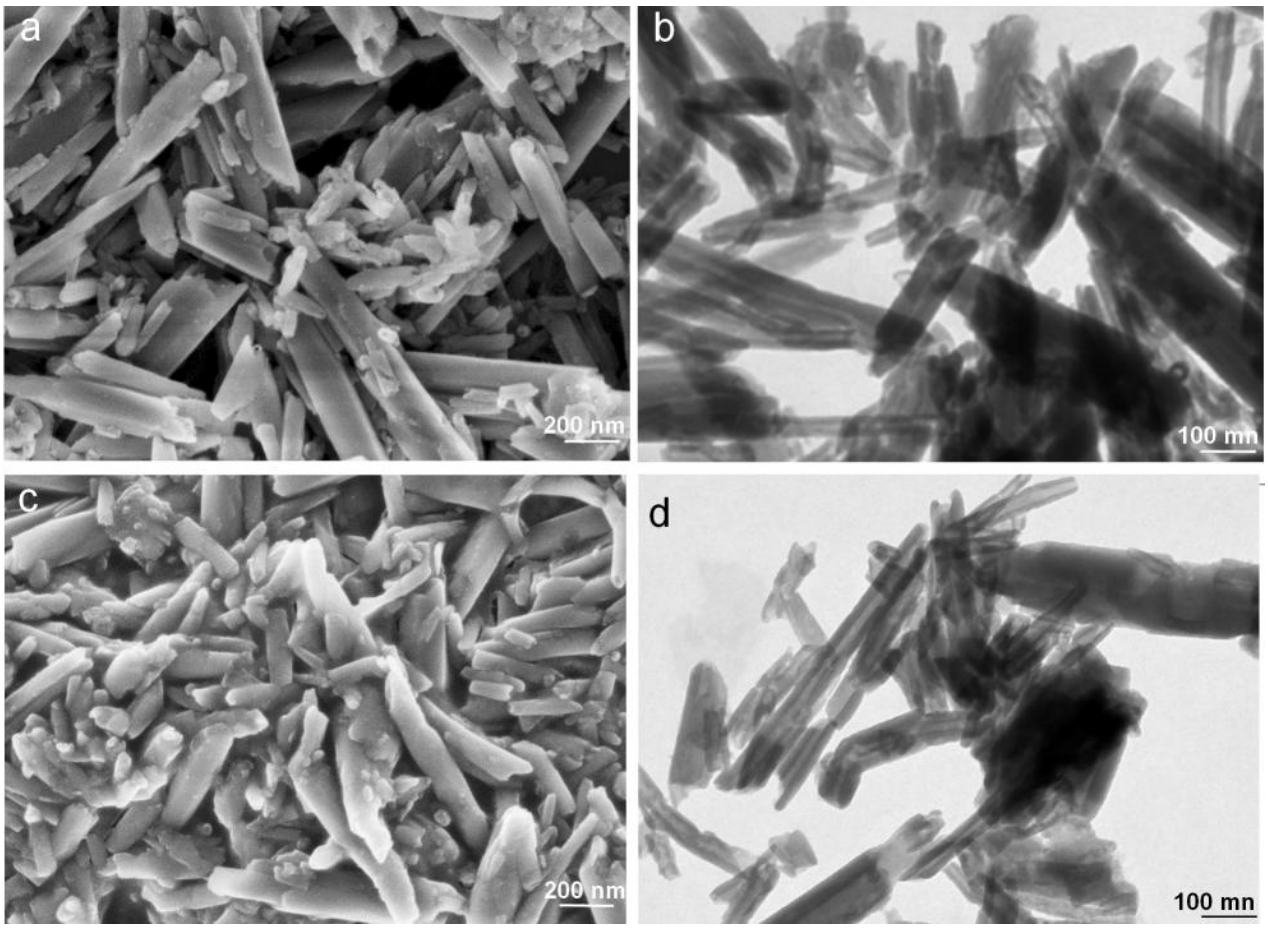

Fig. 20. SEM and TEM images of modified halloysite nanotubes after 3 reaction cycles (a, b) and acid reactivated (c, d)

Thus, the catalytic activity of halloysite nanotubes in the reaction of isopulegol with thiophene-2-carbaldehyde was maintained for at least 3 cycles, practically without affecting the porous structure and acidity. A possibility of acid reactivation was demonstrated, which leads to complete regeneration of the catalytic properties without changing HNT morphology.

Conclusions

In the present work, the catalytic properties of acid-modified halloysite nanotubes (Dragon Mine, USA) were investigated in the Prins reaction of terpenoid (-)-isopulegol with thiophene-2-carbaldehyde to substituted octahydro-2*H*-chromen-4-ol (as 4*R*- and 4*S*-diastereomers). 4*R*-isomer displays high analgesic activity. Active catalysts were obtained by treating halloysite nanotubes (HNT) with 1–30% HCl at 90°C using a rather low acid solution to solid ratio (5 ml per g). The effect of hydrochloric acid concentration on the composition, structure, morphology and acidic properties of halloysite was established using ^{27}Al and ^{29}Si MAS NMR, XRF, N_2 adsorption, FTIR with pyridine, SEM, TEM and thermal analysis. Commercial aluminosilicate catalysts K-10, K-30, AS-36, natural illite as well as scandium triflate and Amberlyst-15 resin were used for comparison.

The reaction was investigated without any solvent and in cyclohexane solution at various concentrations of reactants, temperatures and amounts of catalyst.

It was established that after treatment of halloysite with 5–10% HCl, the concentration of acid sites increased from 34 to 45–52 μmol/g^{-1} though weak acid sites prevailed in all samples. With an increase in the concentration of hydrochloric acid to 20–30%, a decrease in the acidity of materials and almost complete destruction of their tubular morphology with the formation of nanoscale particles of amorphous SiO_2 were observed. The content of Q^3 units (one silica-oxygen tetrahedron is associated with three analogous ones) typical for halloysite decreased from 94.2 to 15.7% with an increase in HCl concentration from 1 to 30%, respectively.

The conditions for halloysite acid treatment (5% HCl) and reaction conditions (temperature 40°C, initial reagents concentration of 0.5 mol/l, air-dry state of the catalyst) were established, allowing an unprecedented high yield (*ca.* 80%) of 4*R*-diastereomer comparable to that for the sum of both isomers on a commercial K-10 clay which is widely used for synthesis of chromene compounds based on terpenoids.

It is shown that the 4*R*/4*S* diastereomers ratio increases from 3.5 to 6.8 as the concentration of acid sites in the catalysts decreases from 153 to 45 μmol·g^{-1}. It has been established that a very high overall selectivity to the desired octahydro-2*H*-chromenol in the presence of halloysite nanotubes (*ca.* 90%) is related to a high ratio of weak to the sum of medium and strong acid sites in them. An increase in selectivity to the dehydration byproducts was observed with an increase in the strength and concentration of acid sites in the studied catalysts.

An increase in the 4*R*/4*S* diastereomer ratio from 3.6 to 6.5 with a decrease in the catalyst drying temperature from 350 to 20°C clearly indicates formation of the 4*R*-isomer in the presence of weak Brønsted acid sites. At the same time, a relatively low selectivity towards chromenol (ca. 25–57%) with a diastereomers ratio of 3.0–3.7 was observed in the presence of strong Lewis (scandium triflate) and Brønsted (Amberlyst-15) acids. According to kinetic modelling, low selectivity to chromenol over strong acidic Amberlyst-15 was due to direct formation of dehydration byproducts from the reactants. For HNT this path was not reliably confirmed whereas exclusively 4*R*-isomer dehydration was observed. The activation energy for 4*R* formation on the halloysite (55±2.1 kJ/mol) was lower than on a previously studied clay (82±1.7 kJ/mol) with a stronger acidity.

Kinetic modelling showed that the order of the catalyst was different for a dried at 110°C resin Amberlyst-15 (1.1±0.12) and air-dry halloysite (1.95±0.09) for the target 4*R*-isomer formation, which clearly indicates the key role of water in the catalytic reaction. Based on the physico-chemical characterization, catalytic tests and kinetic data a mechanism was proposed implying formation of an intermediate with the reagents and transfer of the surface water to the intermediate giving chromenols. A scheme for formation of 4*R*- and 4*S*-diastereomers was proposed.

It has been established that the catalytic activity of halloysite is maintained for at least three reaction cycles without diminishing its acidity, porosity and specific surface area. It was shown that after secondary acid treatment of halloysite the tubular morphology and porous structure were retained.

As a result, novel stereoselective, stable and reusable catalysts for the synthesis of octahydro-2*H*-chromenols were developed allowing an excellent yield of 4*R*-diastereomer under mild reaction conditions. Outstanding selectivity suggests an opportunity for utilization of acid-modified halloysite nanotubes in the synthesis of other heterocyclic compounds through the Prins reaction.

Acknowledgments

The research was financially supported by Belarusian Republican Foundation for Fundamental Research (grant Kh18MS-029). The authors are grateful to Dr. T.F. Kuznetsova and N.V. Kolbun (IGICh of NAS of Belarus) for the performance of N_2 adsorption and XRD analysis. H.P. gratefully acknowledges the financial support of the Ministry of Education and Science of the Russian Federation in the framework of Increase Competitiveness Program of NUST "MISiS" (K4-2017-043).

Conflict of interest

No conflict of interest.

References:

1. R. Pratap, V.J. Ram, Natural and Synthetic Chromenes, Fused Chromenes, and Versatility of Dihydrobenzo[h]chromenes in Organic Synthesis, Chem. Rev. 114 (2014) 10476–10526.

2. N. Majumdar, N.D. Paul, S. Mandal, B. de Bruin, W.D. Wulff, Catalytic Synthesis of 2H-Chromenes, ACS Catal. 5 (2015) 2329−2366.

3. K.U. Sadek, R. A.H. Mekheimer, M. Abd-Elmonem, A. Abdel-Hameed, M.H. Elnagdi, Recent developments in the enantioselective synthesis of polyfunctionalized pyran and chromene derivatives. Tetrahedron: Asymmetry 28 (2017) 1462–1485.

4. O.S. Patrusheva, K.P. Volcho, N.F. Salakhutdinov, Synthesis of oxygen-containing heterocyclic compounds based on monoterpenoids. Russ. Chem. Rev. 87 (2018) 771–796.

5. M. Birringer, K. Siems, A. Maxones, J. Frank, S. Lorkowski, Natural 6-hydroxy-chromanols and -chromenols: structural diversity, biosynthetic pathways and health implications, RSC Adv. 8 (2018) 4803–4841.

6. N. Thomas, S. M. Zacharian, Pharmacological activities of chromene derivatives: An overview, Asian J. Pharm. Clin. Res. 6 (2013) 11–15.

7. E. Nazimova, A. Pavlova, O. Mikhalchenko, I. Il'ina, D. Korchagina, T. Tolstikova, K. Volcho, N. Salakhutdinov, Discovery of highly potent analgesic activity of isopulegol-derived (2R,4aR,7R,8aR)-4,7-dimethyl-2-(thiophen-2-yl)-octahydro-2H-chromen-4-ol, Med. Chem. Res. 25 (2016) 1369–1383.

8. P. N. Moquist, T. Kodama, S. E. Schaus, Enantioselective addition of boronates to chromene acetals catalyzed by a chiral Brønsted acid/Lewis acid system. Angew. Chem. Int. Ed. 49 (2010) 7096–7100

9. N. Casanova, A. Seoane, J.L. Mascareñas, M. Gulías, Rhodium-Catalyzed (5+1) Annulations Between 2-Alkenylphenols and Allenes: A Practical Entry to 2,2-Disubstituted 2H-Chromenes, Angew. Chem. Int. Ed. 54 (2015) 2374–2377.

10. L.F. Silva Jr., S.A. Quintiliano, An expeditious synthesis of hexahydrobenzo[f]isochromenes and of hexahydrobenzo[f]isoquinoline via iodine-catalyzed Prins and aza-Prins cyclization, Tetrahedron Lett. 50 (2009) 2256–2260.

11. A. Macedo, E.P. Wendler, A.A. Dos Santos, J. Zukerman-Schpector, E.R.T Tiekink, Solvent-free Catalysed Synthesis of Tetrahydropyran Odorants: the Role of SiO_2/p-TSA Catalyst on the Prins-Cyclization Reaction J. Braz. Chem. Soc. 21 (2010) 1563–1571.

12. J.S. Yadav, B.V. Subba Reddy, A.V. Ganesh, G.G.K.S. Narayana Kumar, $Sc(OTf)_3$-catalyzed one-pot ene-Prins cyclization: a novel synthesis of octahydro-2H-chromen-4-ols, Tetrahedron Lett. 51 (2010) 2963–2966.

13. S. Slater, P.B. Lasonkar, S. Haider, M.J. Alqahtani, A.G. Chittiboyina, I.A. Khan, One-step, stereoselective synthesis of octahydrochromanes via the Prins reaction and their cannabinoid activities, Tetrahedron Tett. 59 (2018) 807–810.

14. M. Stekrova, P. Mäki-Arvela, N. Kumar, E. Behravesh, A. Aho, Q. Balme, K.P. Volcho, N.F. Salakhutdinov, D.Yu. Murzin, Prins cyclization: Synthesis of compounds with tetrahydropyran moiety over heterogeneous catalysts, J. Mol. Catal. A: Chem. 410 (2015) 260–270.

15. G. Baishya, B. Sarmah, N. Hazarika, An Environmentally Benign Synthesis of Octahydro-2H -chromen-4-ols via Modified Montmorillonite K10 Catalyzed Prins Cyclization Reaction, Synlett. 24 (2013) 1137–1141.

16. M.N. Timofeeva, K.P. Volcho, O.S. Mikhalchenko, V.N. Panchenko, V.V. Krupskaya, S.V. Tsybulya, A. Gil, M.A. Vicente, N.F. Salakhutdinov, Synthesis of octahydro-2H-chromen-4-ol from vanillin and isopulegol over acid modified montmorillonite clays: Effect of acidity on the Prins cyclization. J. Mol. Catal. A: Chem. 398 (2015) 26–34.

17. M.N. Timofeeva, V.N. Panchenko, A. Gil, S.V Zakusin, V.V. Krupskaya, K.P. Volcho, M.A Vicente, Effect of structure and acidity of acid modified clay materials on synthesis of octahydro-2H-chromen-4-ol from vanillin and isopulegol, Catal. Commun. 69 (2015) 234–238.

18. I.V. Ilyina, V.V. Zarubaev, I.N. Lavrentieva, A.A. Shtro, I.L. Esaulkova, D.V. Korchagina, S.S. Borisevich, K P. Volcho, N.F. Salakhutdinov, Highly potent activity of isopulegol-derived substituted octahydro-2H-chromen-4-ols against influenza A and B viruses, Bioorg. Med. Chem. Lett. 28 (2018) 2061–2067.

19. E.V. Nazimova, A.A. Shtro, V.B. Anikin, O.S. Patrusheva, I.V. Il'ina, D. V. Korchagina, V. V. Zarubaev, K. P. Volcho, N. F. Salakhutdinov, Influenza Antiviral Activity of Br-Containing [2R,4R(S),4aR,7R,8aR]-4,7-dimethyl-2-(thiophen-2-yl)octahydro-2H-Chromen-4-ols Prepared from (–)-Isopulegol, Chem. Nat. Compd. 53 (2017) 260–264.

20. N.S. Li-Zhulanov, A.L. Zakharenko, A.A. Chepanova, Ji. Patel, A. Zafar, K.P. Volcho, N.F. Salakhutdinov, J. Reynisson, I.K.H. Leung, O.I. Lavrik, A Novel Class of Tyrosyl-DNA Phosphodiesterase 1 Inhibitors That Contains the Octahydro-2H-chromen-4-ol Scaffold. Molecules 23 (2018) 2468; doi:10.3390/molecules23102468.

21. A.Yu. Sidorenko, A.V. Kravtsova, J. Wärnå, A. Aho, I. Heinmaa, I.V. Il'ina , O.V. Ardashov, K.P. Volcho, N.F. Salakhutdinov, D.Yu. Murzin, V.E. Agabekov, Preparation of octahydro-2H-chromen-4-ol with analgesic activity from isopulegol and thiophene-2-carbaldehyde in the presence of acid-modified clays, Mol. Catal. 453 (2018) 139–148.

22. P. Yuan, D Tan, F. Annabi-Bergaya, Properties and applications of halloysite nanotubes: recent research advances and future prospects, Appl. Clay. Sci. 112–113 (2015) 75–93.

23. P. Pasbakhsh, G.J. Churchman, J.L. Keeling, Characterisation of properties of various halloysites relevant to their use as nanotubes and microfibre fillers. Appl. Clay Sci. 74 (2013) 47–57.

24. E. Joussein, S. Petit, J. Churchman, B. Theng, D. Righi, B. Delvaux, Halloysite clay mineral – a review. Clay Min. 40 (2005) 383–426.

25. G.J. Churchman, P. Pasbakhsh, S. Hillier, The rise and rise of halloysite, Clay Min. 51 (2016) 303–308.

26. Y. Lvov, A. Aerov, R. Fakhrullin, R. Clay nanotube encapsulation for functional biocomposites. Adv. Colloid Interface Sci. 207 (2014) 189–198.

27. L. Zatta, J.E.F. da Costa Gardolinski, F. Wypych, Raw halloysite as reusable heterogeneous catalyst for esterification of lauric acid. Appl. Clay Sci. 51 (2011) 165–169.

28. V.M. Abbasov, H.C. Ibrahimov, G.S. Mukhtarova, E. Abdullayev, Acid treated halloysite clay nanotubes as catalyst supports for fuel production by catalytic hydrocracking of heavy crude oil. Fuel, 184 (2016) 555–558.

29. Z. Zhao, J. Ran, Y. Jiao, W. Li, B. Miao, Modified natural halloysite nanotube solely employed as an efficient and low-cost solid acid catalyst for alpha-arylstyrenes production via direct alkenylation, Appl. Catal. A: Gen. 513 (2016) 1–8.

30. A.Yu. Sidorenko, A.V. Kravtsova, A. Aho, I. Heinmaa, K.P. Volcho, N.F. Salakhutdinov, V.E. Agabekov, D.Yu. Murzin, Acid-modified Halloysite Nanotubes as a Stereoselective Catalyst for Synthesis of 2H-Chromene Derivatives by the Reaction of Isopulegol with Aldehydes. ChemCatChem. 10 (2018) 3950 – 3954.

31. E.P. Barrett, L.G. Joyner, P.P. Halenda, The Determination of Pore Volume and Area Distributions in Porous Substances. J. Am. Chem. Soc. 73 (1951) 373–380.

32. A. Aho, N. Kumar, K. Eränen, T. Salmi, M. Hupa, D.Yu. Murzin, Catalytic pyrolysis of woody biomass in a fluidized bed reactor: Influence of the zeolite structure. Fuel. 87 (2008) 2493–2501.

33. A.Yu. Sidorenko, A.V. Kravtsova, A. Aho, I. Heinmaa, T.F. Kuznetsova, D.Yu. Murzin, V.E. Agabekov, Catalytic isomerization of α -pinene oxide in the presence of acid-modified clays. Mol. Catal. 448 (2018) 18–29.

34. C.A. Emeis, Determination of Integrated Molar Extinction Coefficients for Infrared Absorption Bands of Pyridine Adsorbed on Solid Acid Catalysts. J. Catal. 141 (1993) 347–354.

35. I. Wilson, J. Keeling, Global occurrence, geology and characteristics of tubular halloysite deposits. Clay Min. 51 (2016) 309–324.

36. F. Bergaya, G. Lagaly, Handbook of clay science, Part A: Fundamental, 2013, Elsevier, Amsterdam.

37. P. Komadel, Acid activated clays: Materials in continuous demand. Appl. Clay Sci. 131 (2016) 84–99.

38. P. Yuan, D Tan, F. Annabi-Bergaya, W. Yan, M. Fan, D. Liu, H. He, Changes in Structure, Morphology, Porosity, and Surface Activity Of Mesoporous Halloysite Nanotubes Under Heating, Clays Clay Min. 60 (2012) 561–573.

39. S. Hillier, R. Brydson, E. Delbos, T. Fraser, N. Gray, H. Pendlowski, I. Phillips, J. Robertson, I. Wilson, Correlations among the mineralogical and physical properties of halloysite nanotubes (HNTs), Clay Min. 51 (2016) 325 – 350.

40. E. Abdullayev, A. Joshi, W. Wei, Y. Zhao, Y. Lvov, Enlargement of Halloysite Clay Nanotube Lumen by Selective Etching of Aluminum Oxide, ACS Nano. 6 (2012) 7216–7226.

41. H. He, S. Ji, Q. Tao, J. Zhu, T. Chen, X. Liang, Z. Li, H. Dong, Transformation of halloysite and kaolinite into beidellite under hydrothermal condition, American Mineralogist, 102 (2017) 997–1005.

42. H. He, J. Guo, X. Xie, H. Lin, L. Li, A microstructural study of acid-activated montmorillonite from Choushan, China, Clay Min. 37 (2002) 337–344.

43. V.A. Drits, B.A. Sakharov, S. Hillier, Phase and structural features of tubular halloysite (7Å), Clay Min. 53 (2018) 691–720.

44. M. Guisnet, P. Ayrault, C. Coutanceau, M.F. Alvarez, J. Datka, Acid properties of dealuminated beta zeolites studied by IR spectroscopy, J. Chem. Soc., Faraday Trans. 93 (1997) 1661–1665.
45. R.E. Grim, Clay Mineralogy, New York: McGraw-Hill, 1968.
46. D. Garcia-Garcia, J.M. Ferri, L. Ripoll, M. Hidalgo, J.Lopez-Martinez, R. Balart, Characterization of selectively etched halloysite nanotubes by acid treatment, Appl. Surf. Sci. 422 (2017) 616–625.
47. R.D. White, D.V. Bavykin, F.C. Walsh, The stability of halloysite nanotubes in acidic and alkaline aqueous suspensions. Nanotechnology, 23 (2012) 065705.
48. O.S. Mikhalchenko, D.V. Korchagina, K.P. Volcho, N.F. Salakhutdinov, A practical way to synthesize chiral fluoro-containing polyhydro-2H-chromenes from monoterpenoids, Beilstein J. Org. Chem. 12 (2016) 648–653.
49. P. Borkar, P. van de Weghe, B.V.S Reddy, J.S. Yadav, R. Grée, Unprecedented synergistic effects between weak Lewis and Brønsted acids in Prins cyclization. Chem. Commun. 48 (2012) 9316 – 9318.
50. M. Breugst, R. Grée, K.N. Houk, Synergistic Effects between Lewis and Brønsted Acids: Application to the Prins Cyclization, J. Org. Chem. 78 (2013) 9892–9897.
51. S. Yariv, H. Cross, Organo-Clay Complexes and Interactions. Marcel Dekker, New York, 2002.
52. D.Yu. Murzin I.L. Simakova J.Wärnå, Selectivity Analysis for Networks Comprising Consecutive Reactions of Second and First Order. Int. J. Chem. React. Eng. Published Online: 2018-09-28, DOI: https://doi.org/10.1515/ijcre-2018-0161
53. J. Burés, A Simple Graphical Method to Determine the Order in Catalyst. Angew. Chem. Int. Ed., 55 (2016) 2028–2031.
54. H. Haario, ModEst, Modelling and optimization software, Helsinki, 2011.
55. S. Wang, E. Iglesia, Mechanism of Isobutanal − Isobutene Prins Condensation Reactions on Solid Brønsted Acids, ACS Catal. 6 (2016) 7664 – 7684.